This is to certify that the

thesis entitled

Impact Testing of Navy Bean Pods

presented by

Nor Mariah Adam

has been accepted towards fulfillment
of the requirements for

M.S. degree in Agricultural Engr.

Thomas H Burkhardt

Major professor

Thomas H. Burkhardt

Date 5/20/85

IMPACT TESTING OF NAVY BEAN PODS

by

Nor Mariah Adam

A THESIS

Submitted to
Michigan State University
in partial fulfillment of the requirements
for the degree of

MASTER OF SCIENCE

Department of Agricultural Engineering

1985

Nor Mariah Adam

Approved: Thomas H Burkhardt
Major Professor

Approved: Donald C McElwain
Department Chairman

ACKNOWLEDGEMENTS

The author wishes to express sincere gratitude to the following:

Dr Thomas H. Burkhardt (Agricultural Engineering) for his advise, encouragement and suggestions as major adviser;

Dr. George Mase (Metallurgy, Mechanics and Materials Science) and Dr. James D. Kelly (Crop and Soil Science) for their time, constructive criticism and moral support;

Mr. Gary Connor and Pedro Herrara for helping with the construction of equipment, and Abdul Razak Habib for helping with the experimental design, statistical analysis and computer work;

Staff and students in the Department of Agricultural Engineering for their helpful support in the course of this study;

Last but not least, her parents, Encik Adam Abdul Aziz and Puan Azizun Dahalan for their unfailing love, encouragement and faith in their daughter's pursuit for knowledge.

TABLE OF CONTENTS

LIST OF TABLES

LIST OF FIGURES

ABSTRACT

IMPACT TESTING OF NAVY BEAN PODS

by

Nor Mariah Adam

A pendulum system was developed for impacting 1983 and 1984 Swan Valley and C-20 navy bean pods. The impulse, maximum impact force and energy absorbed to shatter were measured. A 2x3x3 factorial design at 2 levels of variety, 3 levels of pendulum release angle and 3 pod positions (side, top, base) was used.

The mean absorbed energy was 10.16 mJ with a range of 1.40-31.50 mJ, the mean maximum impact force value was 24.82 N with a range of 11.32-36.97 N and the mean impulse value was 24.32 N-ms with a range of 6.04-71.67 N-ms. Impulse and absorbed energy to shatter depend on pod orientation. The bean pod is weakest when it is hit along the base. Impulse is the most suitable parameter to characterize impact resistance because it is dependent on pod orientation and independent of variety, time of harvest and pendulum release angle.

CHAPTER I

INTRODUCTION

1.1 Background

Michigan has been a leading producer of navy beans. In 1983 over 80 percent of the navy beans produced in the United States were grown in Michigan, which was equivalent to a crop value of about 110 million dollars (Michigan Agricultural Statistics, 1984).

The current method of harvesting navy beans in Michigan is by windrow harvesting (Kelly, Burkhardt, Varner, Adams and Srivastava, 1981). This method of harvest involves two operations. Early in the morning when the beans are damp, a bean puller pulls the plants from the ground and forms windrows. The windrows are then left to dry in the sun. Later in the day, a combine harvester collects the windrows to harvest the crop.

Usually navy bean harvest starts in middle September and continues into early October. In Michigan this is the time of year when foggy nights and high humidity days are common. If the grower pulls more beans in the morning than can be harvested in the afternoon, some windrowed beans must be left in the field for harvest at a later time. If

rains come before these windrowed beans can be harvested, they will be more severely damaged than bean plants which are still standing in the field. If the grower pulls too few plants, he reduces the length of his effective harvest day. Indeed direct combining of navy beans was a salvage operation for the wet seasons of 1975 and 1977 because fields were too wet for conventional harvest (Pickett, 1982).

The advantages of direct combining navy beans have been realized by farmers as early as 1952 (Khan, 1952). In windrow harvesting losses from shelling, machine damage and degradation are common when windrowed beans are exposed in wet weather (Gunkel and Anstee, 1962). Direct harvesting on the other hand, is a one-step operation. Merits of direct harvesting mentioned by Kelly et al. (1981) are as follows:

i. standing plants dry faster than windrowed plants, so combining can begin earlier in the day,
ii. eliminates the need for guessing the hectares of crop to be pulled in the morning,
iii. the grower can continue to harvest the crop until the beginning of a rainstorm,
iv. direct harvesting requires less equipment, hence operation cost is lower,
v. a combine harvester has better floatation on wet soil than a tractor-mounted bean puller, which tends to

bury more beans during the pulling operation for wet soil conditions.

1.2 Bean Plant

According to Kelly and Adams (1981), major navy bean plant types grown commercially in Michigan are as follows:

i. bush type

ii. short vine type

iii. vine type

Since 1973, the navy bean breeding program at Michigan State University has been working towards the development of the taller, narrow profile and more erect plant type called architypes (Adams, 1981). Architypes are modified bush type and short vine type navy bean plants. For example, C-15 is an upright bush type variety while Swan Valley is an upright short vine type variety (Kelly and Adams, 1981).

Architypes have been developed using parental stocks which were more tolerant to air pollution and soil compaction as compared to the standard bean varieties. They can be grown in narrower rows than the usual 71 to 76 cm (28 to 30 inches), resulting in a higher plant density which leads to a higher yield per unit area (Adams, 1981).

The architype bears bean pods which grow well above the ground and these pods mature uniformly. The stem is erect and has a high resistance to lodging. These

characteristics make architypes ideal for direct harvest. In addition, the erect and narrow profile appears to create less favorable humidity conditions for white mold growth (Adams, 1981).

1.3 Anatomy of Bean Pod

In North America, beans are classified under the genus Phaseolus. Most of the common dry edible beans like kidney beans, navy beans, pinto beans and snap beans belong to the varietal classification Phaseolus Vulgaris L. (Narayan, 1969). Figure 1.1 shows a picture of whole and opened navy bean pods. Usually there are six or seven seeds in a navy bean pod. Pod dimensions vary with different seed size and class. For example, navy bean mass is 20 g per 100 seeds while kidney bean mass is 60 g per 100 seeds (Kelly, 1984).

Beans belong to the legume family and they possess dry dehiscent (or self-exploding) pods. The exocarp, which includes the epidermal layer and the subepidermal layer, is composed of thick walled cells (Esau, 1960). Figure 1.2 shows a transverse section of a Phaseolus pod. From the diagram, it can be seen that the seed is attached to the pod suture by the fine funicle.

Differential shrinkage of different tissues in the pericarp of a legume, is assumed to be the primary force inducing split in longtitudinal dehiscence (Esau, 1953). When the pericarp splits, the two valves of the dried

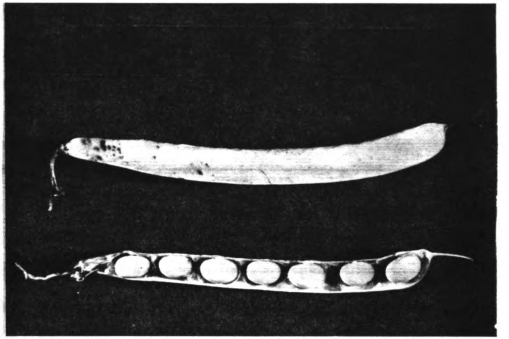

Figure 1.1 Picture of Whole and Opened Navy Bean Pods

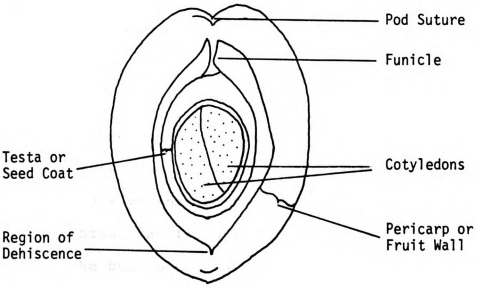

Figure 1.2 Transverse Section of A Phaseolus Pod (From An Atlas of Plant Structure Vol. 2, by Bracegirdle and Miles, 1973)

legume twist, thereby expelling the seeds.

1.4 Shatter

Shatter is the splitting of the bean pod. During harvesting, shatter can occur when the cutter bar cuts into the bean pod, causing the pod to pop open, thereby releasing the seeds. Kelly et al. (1981) defined shatter loss as "...loose beans and beans in pod not attached to plant.." which were on the soil surface, excluding the preharvest losses. In this study the focus is on loose beans and not loose pods and the criteria for pod shatter is when one or more seeds pop out of the bean pod after impact. Shatter is brittle failure of the bean pod (Hoag, 1975). In engineering, material properties related to brittle failure include ultimate strength and strain energy. It is then possible to know the parameters related to pod shatter when the pod's engineering properties are known.

It has been observed that the amount of elapsed time between maturity and harvest affects shatter loss for both navy beans and soybeans (Singh, 1975 and Hoag, 1975). Hoag (1975) suggested that fatigue, caused by cyclic wetting and drying of the bean pods, may contribute to the increase in shatter loss.

One of the ways to reduce field shatter loss is by developing suitable varieties. Indeed shatter resistance

has been used as a criterion in the selection of soybean varieties (Hoag, 1975).

1.5 Objective

The purpose of this work is to build a portable machine for finding physical properties of navy bean pods. Specific objectives are:

i. To find pod orientation most susceptible to shatter,

ii. To measure the impulse required to initiate shatter,

iii. To measure the energy absorbed by the bean pod during impact,

iv. To use the above information to find the parameter most suitable to characterize impact resistance for variety development.

CHAPTER II

REVIEW OF LITERATURE

According to Mohsenin (1978), mechanical damage is a by-product of mechanizing harvesting and handling of agricultural products. Impact is a major cause of mechanical damage in harvesting and subsequent processing and handling operations (Fluck and Ahmed, 1973). Product damage like bruises, burst or split fruit, can lead to significant economic losses during storage, handling and marketing of agricultural products (Finney and Massie, 1975). It has been found that some crop varieties are more susceptible to impact damage than others (Hoag, 1973 and Mohsenin, 1978). This offers an opportunity for plant breeders to develop new varieties which would withstand the mechanical force imposed during production.

2.1 Some Parameters Related to Seed and Grain Damage

Common experimental variables used in the analyses of seed and grains subjected to impact are as follows:

i. impact velocity

ii. moisture content

iii. product orientation.

The common measured quantities are

i. imparted impulse

ii. energy absorbed to initiate damage

iii. peak resistive force.

Bilanski (1966) analyzed damage resistance of various seed grains under gradually applied load, as well as under low and high impact velocities. He found damage resistance dependent on grain size, moisture content and grain orientation. He also observed that grains with high moisture content required more energy to initiate damage than low moisture grains. Perry and Hall (1966) also found impact velocity, moisture content and product size influenced damage resistance when they dropped navy beans at various heights in a silo. In addition to these factors, they found that temperature also influenced damage.

Turner, Suggs and Dickens (1967) varied impact velocity, moisture content and specimen orientation in their impact experiment on peanuts. They found the coefficient of restitution depended on specimen orientation. When low moisture peanuts were subjected to high impact velocities, they observed that these peanuts were mostly damaged by the brittleness of the hulls. Hoag (1972) used experimental variables similar to Turner et al.'s (1967) for his impact experiment on soybean pods. Contrary to Turner et al.'s finding, Hoag (1972) found that

specimen orientation did not give significant differences in energy adsorption to initiate pod shatter. Hoag (1975) extended his research and found that the maximum force to cause soybean pod damage dependent on the pod moisture content. He recommended imparted impulse to be used as an indicator of field shatter loss.

Reported studies on corn breakage due to impact were mainly concerned with defining parameters that can characterize corn kernel resistance to shearing. Srivastava, Herum and Stevens (1976) impacted corn kernels at various orientations and moisture levels. They measured maximum resistive force, imparted impulse and energy absorbed to initiate failure. They found, generally, that these values increased with moisture content. They recommended energy absorbed per unit area in longtitudinal impact to characterize impact strength of corn kernels. Mensah, Herum, Blaisdell and Steven (1981) obtained similar measured quantities as Srivastava et al. (1976) for their impact experiment on corn kernel. Although they obtained general observations similar to Srivastava et al. (1976), they recommended the peak shear stress to characterize impact strength of corn kernels.

2.2 Previous Research Work on Navy Beans in Michigan

Post war research on navy beans were mainly concerned with improving harvesting techniques (Khan, 1952).

Research on direct harvesting of the bush type navy beans in the early 1950's has been reported (Mc Colly, 1958). Mc Colly (1958) found that the finger type reel was more efficient than the standard bat type. This is because the tines on the finger type reel could be adjusted such that the bean plants were lifted towards the cutter bar, thereby reducing cutter bar losses and shatter losses. He also mentioned that the available plant variety at that time was not suitable for direct harvesting.

Some research related to navy bean harvesting has dealt with the pod moisture content. Pickett (1973) found mechanical damage to navy beans during harvesting dependent on both pod and seed moisture content as well as on the cylinder speed. He also stated that pod moisture content was likely to affect threshability. For optimum harvest conditions, he recommended a moisture content of under 12 percent for the bean pod and between 17 and 20 percent for the bean seeds. Singh (1975) studied the Sanilac and Seafarer navy bean varieties to evaluate environmental effects on field drying and harvesting. He developed models for rate of change of moisture levels and overnight rise in moisture level for both bean pods and bean seeds separately. He also developed a model for unthreshed loss as a function of pod moisture content and cylinder speed. Since the models indicated varietal differences, he suggested that physical properties of newly introduced

varieties be found before using his prediction models. He agreed with Pickett (1973) that threshability of the crop was influenced by the bean pod moisture content. For maximum threshability with minimum bean damage, Singh (1975) recommended moisture levels of under 13 percent for the bean pod, and between 18 and 20 percent for the bean seeds.

Knowledge about physical and mechanical properties of navy bean seeds is important for seed production and processing; and for reduction in seed damage during harvesting and handling operations. Reported research on the determination of these properties was done under quasi-static and/or impact loading.

Perry and Hall (1965) used a wooden bar to strike individual navy bean seed at various moisture levels and various impact velocities. These velocities were similar to velocities that would have been attained by the navy beans after a free fall of 6.1 to 7.6 meters (20 to 25 feet). They used high speed photography to evaluate the impact force, impact duration and deformation of each seed. Narayan (1969) used the column stability theory to compute stability modulus and elastic modulus of navy bean seeds under quasi-static loading. He used a high velocity impact arm to measure impact forces required to cause seed checking. Checking is splitting of the seed coat. Hoki (1973) measured Young's modulus and ultimate strength of

navy bean seed coat and cotyledons separately under quasi-static tensile loading. He used the contact theory to predict deformation of the navy bean seed under compressive loading. The contact theory was incorporated with the impact theory to predict damage under impact loading.

2.3 Measurement of Mechanical Properties of Biological Materials.

Several types of measuring techniques have been developed for specific agricultural products. Uniformity in testing techniques is difficult because of the complex structure and variations in size and shape of agricultural products. To date, only the Stein tester is commercially used to test mechanical strength of grains (Singh and Finner, 1983).

Measuring techniques can be divided into quasi-static and dynamic methods. Common quasi-static loading is either under compression loading or tension loading. Tension testing is less popular due to the difficulty in gripping the specimen without damaging the tissues. Dynamic testing includes simple drop tests, pendulum, pneumatic impact device, rotary arm, centrifugal impactor and vibration tests.

Simple drop tests, either of a product upon a rigid surface, or of a mass upon the product, have been

extensively used (Perry and Hall, 1966; Hammerle and Mohsenin, 1966; Sharma and Bilanski, 1971 and Fluck and Ahmed, 1973). With this method, the velocity at impact is limited by the drop height and orientation of a dropped specimen is impossible to control.

The pendulum is a popular impacting device (Perry and Hall, 1965; Bilanski, 1966; Turner et al., 1967; Hoag, 1972; Srivastava et al., 1976 and Mensah et al., 1981). The pendulum is versatile; the impact velocity can be varied either by changing the pendulum length (Lyon and Zable, 1973) or by changing the release angle (Bilanski, 1966 and Srivastava et al.,1976). This method allows easy control of specimen orientation.

High velocity impact arms driven by variable speed motors have been employed for high speed impact testing (Bilanski, 1966; Turner et al., 1967 and Burkhardt and Stout, 1971). This method is used to simulate free impacts during threshing or handling.

Keller, Converse, Hodges, and Do Sup Chung (1972) evaluated corn kernel damage by pneumatically projecting the kernels against selected materials. Hoki and Pickett (1973) developed a high speed impact tester which consisted of a rotating impact disk and a vacuum bean holding disk. The centrifugal impactor has been used to provide random impacts under controlled speeds for corn kernels and soybean seeds (Cooke and Dickens, 1971; Paulsen, Nave and

Gray, 1981 and Singh and Finner, 1983).

Vibrational characteristics of agricultural products have to be known before vibratory harvesting can be done. Research has been done on the mechanical impedance of blueberries (Rohrbach and Glass, 1980), the vibrational characteristics of blueberry canes (Ghate and Rohrbach, 1975) and the resonant frequencies of strawberries (Idell, Holmes and Humphries, 1975).

2.4 Instrumentation Methods

High speed photography is a popular method of measuring the impact velocity of a pendulum (Perry and Hall, 1965; Turner et al., 1967; Hoag, 1972 and Burkhardt and Stout, 1974). This method gives a continuous documentation of impact and allows an accurate and reliable way to measure impact duration. Careful coordination of film exposure rate with the impacting arm movement is important. Precaution must be taken to prevent the specimen from drying under the heat of the camera lights. Perry and Hall (1965) used an asbestos shield to protect their specimens from the heat of the camera lights.

The piezo-electric or quartz type accelerometer has been used for continuous measurement of acceleration (Hammerle and Mohsenin, 1966; Burkhardt and Stout, 1971; Hoag, 1972; Lyon and Zable, 1973; Fluck and Ahmed, 1973; Srivastava et al., 1976 and Mensah et al., 1981). The

acceleration signal is usually preamplified and is commonly displayed on a storage oscilloscope.

An angular transducer, such as a tachometer transducer or a shaft encoder, may give a continuous measurement of the pendulum angular position (Bilanski, 1966 and Mensah et al. 1981). It is convenient to have the angular transducer output displayed on a chart recorder.

Strain gauges have many applications in experimental work. Bledsoe and Swingle (1972) measured detachment properties of snap beans using strain gauges attached on a cantilever. Goyal, Drew, Nelson and Logan (1980) used strain gauges to evaluate seed emergence forces. The strain gauges were placed on an aluminium ring which acted as a sensing element. The force transducer was sensitive enough to measure forces to the nearest 0.01 N.

2.5 Summary

Product damage can be reduced in today's mechanized production of agricultural products, when the physical properties of the products are known. Several types of measuring techniques and instrumentation exist because of variations in product size, shape and complex structure. Common parameters to characterize impact strength are imparted impulse, peak resistive force and energy absorbed to initiate damage. Common measuring techniques are quasi-static loading, pendulum, simple drop tests,

pneumatic impact device, high velocity impact arm, centrifugal impactor and vibration tests. Popular instrumentation techniques uses the accelerometer, shaft encoder and strain gauges.

CHAPTER III

THEORETICAL CONSIDERATIONS AND EXPERIMENTAL DESIGN

3.1 Theoretical Considerations

Characteristics of an acceleration-time or force-time curve are important for analysis of impact. Hammerle and Mohsenin (1966) stated that absorbed energy and duration of impact are important factors to initiate impact damage. It is also possible to determine the type of damage from the force-time curve (Fluck and Ahmed, 1973).

3.1.2 Impact Energy

For a pendulum with no input power, as in Figure 3.1, impact energy is provided by the gravity field to the pendulum mass, and is a function of the release height. By the Law of Conservation of Energy, the total energy, that is the sum of kinetic energy T, plus the potential energy V, remains constant up to the instant of impact. In equation form,

$$T_1 + V_1 = T_2 + V_2$$

where the subscripts refer to arbitrary positions of the pendulum prior to impact.

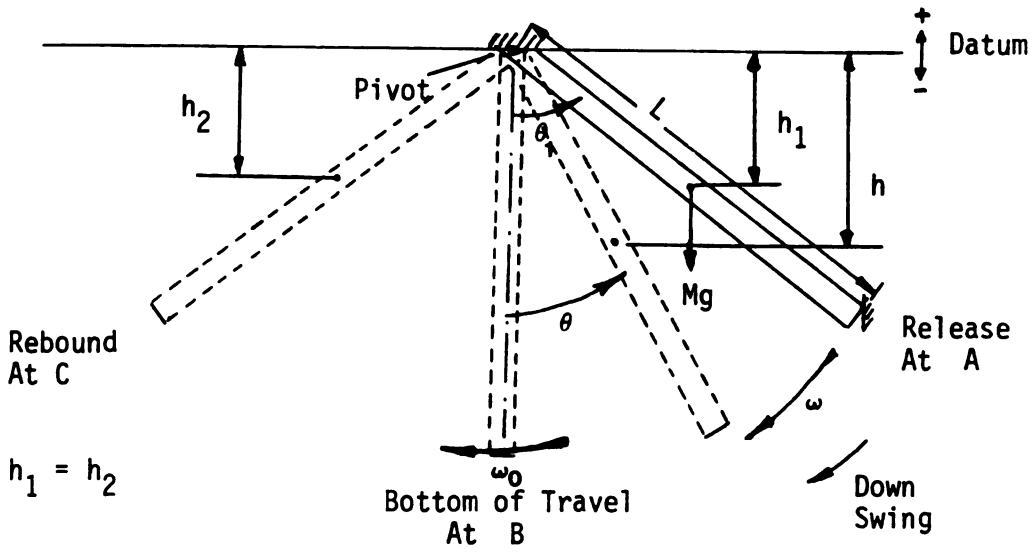

Figure 3.1 Sketch of A Pendulum Without Input Power and Without Specimen (no impact)

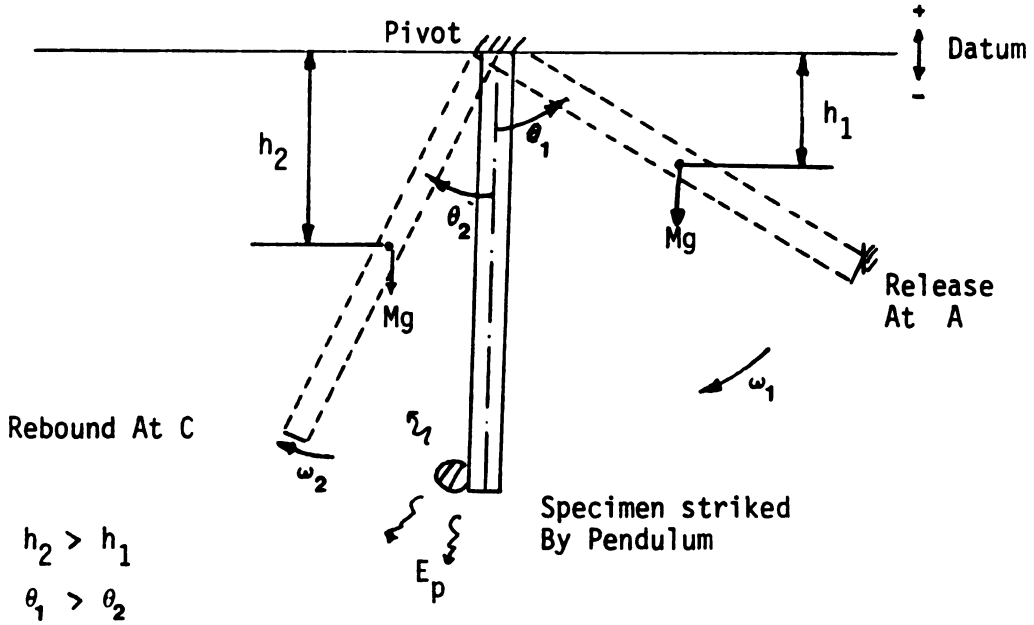

Figure 3.2 Sketch of Pendulum Without Input Power With Specimen (with impact)

3.1.2.1 Without Specimen (No Impact)

With no impact, the total energy at A equals the total energy at all positions of the down swing, including at the bottom of travel (See Figure 3.1). This can be expressed as:

$$T_A + V_A = T_{AB} + V_{AB} = T_B + V_B$$

where:

subscript A refers to position at A,

subscript AB refers to position between A and B,

subscript B refers to position at B.

Substitution in the above equation yields:

$$0 + Mg(L-h_1) = 1/2\ I_0\omega^2 + Mg(L-h) = 1/2\ I_0\omega_0^2 + Mg(L - L/2)$$

which simplifies to:

$$0 - Mgh_1 = 1/2\ I_0\omega^2 - Mgh = 1/2\ I_0\omega_0^2 - Mg\ L/2 \qquad (3.1)$$

where:

Mg - weight of the pendulum, N,

h_1 - position of the pendulum center of gravity at A (at release), m,

I_0 - mass moment of inertia about pivot, $kg\text{-}m^2$,

ω - angular velocity at an arbitrary position between A and B, rad/s,

h - position of pendulum center of gravity at an arbitrary position between A and B, m,

ω_0 - angular velocity at bottom of travel, rad/s,

L - length of pendulum arm, m.

From Equation 3.1 we get:

$$Mg\ (\ h - h_1\ ) = 1/2\ I_0\omega^2 \qquad (3.2)$$

$$Mg\ (L/2 - h_1\ ) = 1/2\ I_0\omega_0^2 \qquad (3.3)$$

Additionally, with no specimen in the fixture, and hence no impact, energy will be conserved between position A and position C. Here

$$T_A + V_A = T_C + V_C$$

or $$0 - Mgh_1 = 0 - Mgh_2$$

so that, for a completely frictionless pendulum, $h_1 = h_2$. However, experimentally $h_2 > h_1$ because of the presence of friction in the pivot bearing. Therefore, if h_1 and h_2 can be measured, for a range of values of h_1, the corresponding friction values can be calculated.

3.1.2.2 With Specimen (With Impact)

When the pendulum strikes the specimen (bean pod), as in Figure 3.2, the motion of the pendulum can be divided into three parts, namely:

i. down swing,

ii. impact (negligible motion of the pendulum),

iii. up swing.

Down Swing

Applying Equation 3.1, the total energy at pendulum release and <u>just</u> prior to impact can be written in the energy balance equation as:

$$0 - Mgh = 1/2\ I_0\omega_1^2 - Mg\ L/2$$

where ω_1 is the angular velocity just before impact in rad/s. The above equation can be simplified to give a general equation before impact as

$$Mg\ (L/2 - h_1) = 1/2\ I_0\omega_1^2 \qquad (3.4)$$

Impact

When the pendulum hits the specimen, some energy will be absorbed by the bean pod. The absorbed energy may appear as some form of damage to the bean pod. Equation 3.1 then becomes

$$T_C + V_C = T_B + V_B \qquad \text{(just after impact)}$$

or $$0 - Mgh_2 = 1/2\ I_0\omega_0^2 - Ep - Mg\ L/2 \qquad (3.5)$$

where Ep is the energy absorbed by the bean pod during impact and h_2 is the pendulum center of gravity at C. Substitution of Equation 3.3 into Equation 3.5 yields

$$Ep = Mg\ (h_2 - h_1) \qquad (3.6)$$

and $h_2 > h_1$.

Up Swing.

During impact some energy is transferred to the bean pod. Following impact, the Law of Conservation of Energy holds for the up swing motion. The total energy at the bottom of travel equals the total energy at the end of the up swing, C. The energy equation can be written as:

$$0 - Mgh_2 = 1/2\ I_0\omega_2^2 - Mg\ L/2$$

where ω_2 is the angular velocity after impact in rad/s. The above equation can be simplified to give a general equation after impact as:

$$Mg\ (L/2 - h_2) = 1/2\ I_0 \omega_2^2 \qquad (3.7)$$

Equations 3.4 and 3.7 are the energy balance equations for conditions before and after impact. Clearly, the difference in energy levels before and after impact is attributed to the energy transferred to the bean pod during impact. In equation form,

$$1/2\ I_0 (\omega_1^2 - \omega_2^2) = Ep = Mg\ (h_2 - h_1) \qquad (3.8)$$

The value of the energy absorbed by the bean pod during impact, Ep, can be computed when both ω_1 and ω_2, or both h_1 and h_2 are known. From trigonometry,

$$h_1 = L/2 \cos \theta_1$$

and

$$h_2 = L/2 \cos \theta_2, \quad \theta_1 > \theta_2 \qquad (3.9)$$

where θ_1 and θ_2 are the release angle and the maximum rebound angle respectively.

The impact motion can also be graphically described by the angular velocity, ω, versus the position of the pendulum center of gravity, h, as in Figure 3.3. Between A and B is the region of downswing, and at impact BB', some energy is transferred to the bean pod during a very short period of time. This is characterized by the sudden decrease in ω. Between B' and C is the region of upswing after impact. Clearly, due to the energy transfer to the

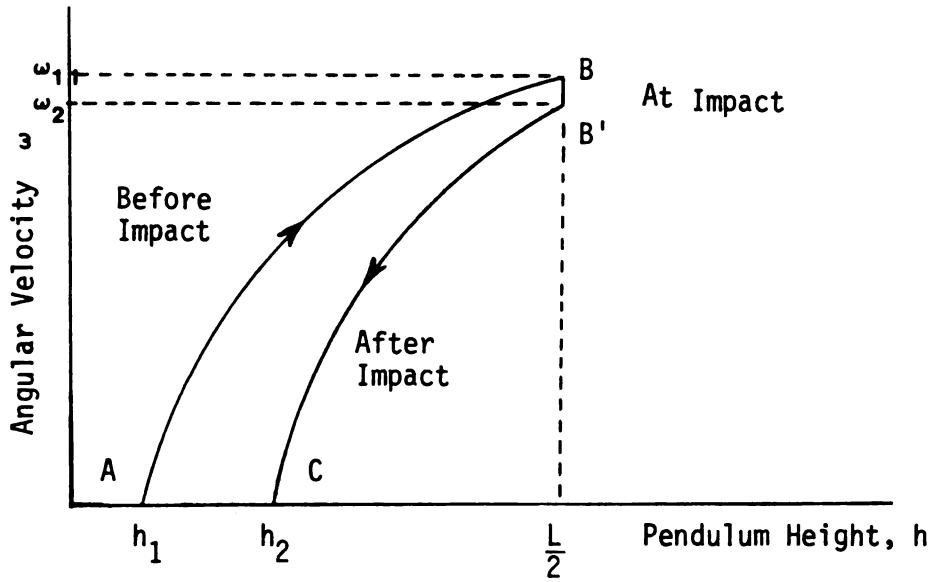

Figure 3.3 Graph of Angular Velocity ω versus Pendulum Height h for A Pendulum Impacting A Specimen

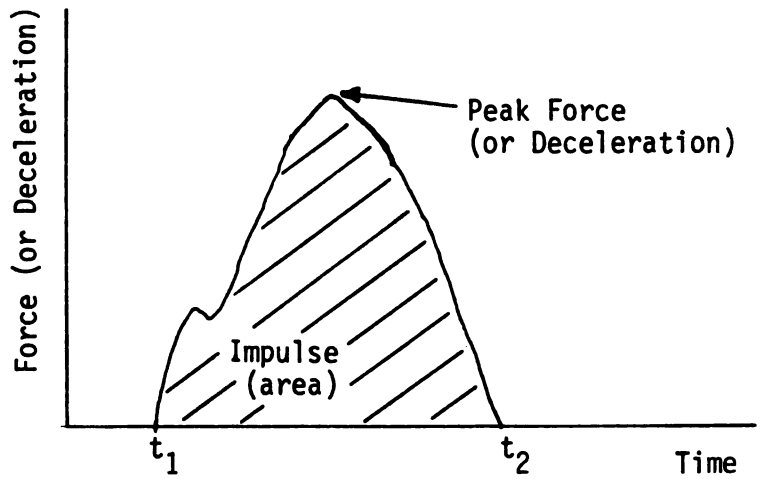

Figure 3.4 Typical Force-Time or Deceleration-Time Curve For A Fruit or Vegetable with A Non-Yielding Surface (From Fluck and Ahmed, 1973)

bean pod, the motion ends at h_2, where $h_2 > h_1$.

The values of ω for conditions before impact can be computed using Equation 3.2, where the ω^2 term can be simplified to give

$$2\ Mg/I_0 * (h - h_1) = \omega^2$$

This can be written as

$$\omega = \sqrt{2Mg(h - h_1)/I_0} \qquad (3.10)$$

From Equation 3.10 it is possible to get a plot of ω for a range of values of h.

3.2 Impact Action

According to Mohsenin (1978), the concept of impulse-momentum forms the classical theory of impact. From Goldsmith (1960), the Linear Impulse-Momentum Law is given by:

$$\int_0^t F\ dt = \int_0^v d(mv) \qquad (3.11)$$

where:

F - impact force, N,

t - duration of impact, s,

v - linear velocity, m/s,

m - mass of object, kg.

For a constant mass, from Turner et al. (1967), Equation 3.11 becomes

$$\int_0^t F\,dt = mp \int_0^{vp} dv = mp\ vp \qquad (3.12)$$

where:

mp - mass of bean pod, kg,

vp - linear velocity of bean pod just after impact, m/s.

A typical curve such as in Figure 3.4 can be obtained by an instrumented target with which the specimen collides (Fluck and Ahmed, 1973). The peak force is the highest point on the curve. The impact duration, $t_2 - t_1$, is the time interval between the initiation and the termination of impact. The area under the force-time curve is the experimental impulse value.

High speed photography can be used to verify velocity calculations and to determine specimen deformation.

3.3 Experimental Design

In this study three factors of interest were variety, pod orientation and pendulum release angle. These variables are independent of each other. Variety and pod orientation are qualitative factors while the release angle is a quantitative factor. Two bean varieties were tested, which means that variety was a two-level factor. Both pod orientation and release angle were three-level factors.

The factorial treatment combination of 2 x 3 x 3 is shown in Table 3.1. This type of treatment combination allows one or both of the following analyses to be performed:

i. Computation of main effects and interaction between factors,

ii. Identification of factors that can lead to future work.

A random complete block design was used with time as the blocking factor. This means that within a particular block of time, the bean pods were subjected to all 18 treatment combinations. Each experimental unit was subjected to a particular treatment combination, which was chosen at random.

Moisture content was not included as a fourth factor so as to increase the precision of the statistical tests. A 2x3x3x3 factorial treatment combination with moisture content at three levels would require 54 treatment combinations. This is not possible due to the limited number of bean pods available and the size of work anticipated.

Table 3.1 A 2x3x3 Factorial Combination Table

Run	Variety	Release angle	Pod orientation
1	C-20	40	top
2	C-20	40	bottom
3	C-20	40	lateral
4	C-20	50	top
5	C-20	50	bottom
6	C-20	50	lateral
7	C-20	60	top
8	C-20	60	bottom
9	C-20	60	lateral
10	Swan Valley	40	top
11	Swan Valley	40	bottom
12	Swan Valley	40	lateral
13	Swan Valley	50	top
14	Swan Valley	50	bottom
15	Swan Valley	50	lateral
16	Swan Valley	60	top
17	Swan Valley	60	bottom
18	Swan Valley	60	lateral

CHAPTER IV

EQUIPMENT

A pendulum system was set up as shown in Figure 4.1, to impact navy bean pods. The system was comprised of:

i. a pendulum

ii. bean pod holders

iii. electrical release mechanism

iv. angular transducer and counter timer

v. force transducer

vi. storage oscilloscope with special camera.

4.1 Pendulum

The pendulum, a modified steel bar, was supported on two ball bearings. A pointer was placed at the top of the pendulum to read off the angle on the graduated angle plate (protractor) for measurement of release angle, rebound angle and angular speed of the pendulum.

4.2 Bean Pod Holders

The bean pod holders were screwed into supports in a stand (See Figure 4.2). The bean pod was simply supported on the holders such that the pod could be fixed at any

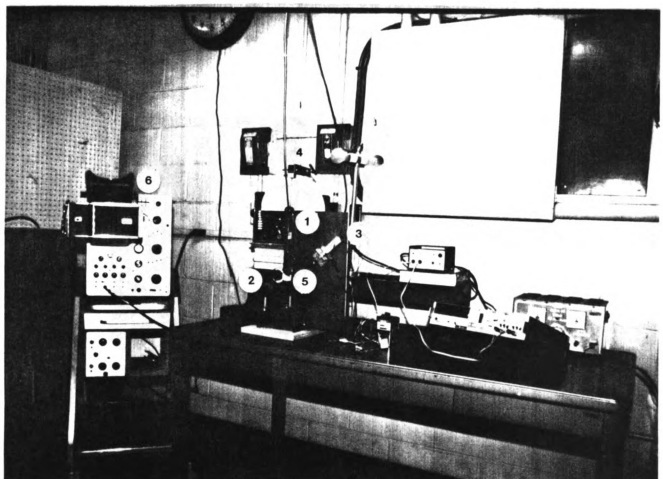

Figure 4.1 Equipment Assembly for Impact Testing of Navy Bean Pods
1. Pendulum 2. Bean Pod Holders 3. Electrical Release Mechanism
4. Angular Transducer 5. Force Transducer 6. Storage Oscilloscope
With Camera in Position

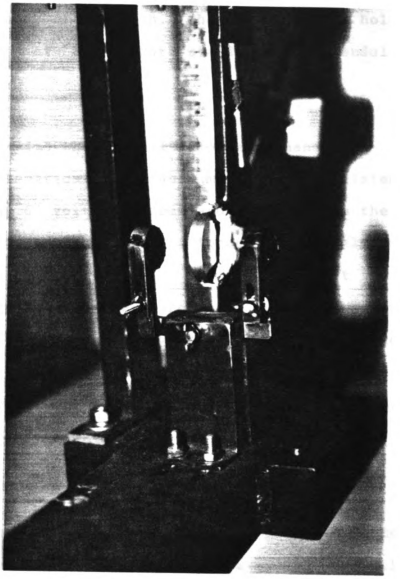

Figure 4.2 Bean Pod Holders

orientation to the impacting ring, and moved to any position along its length. The height of the holders and the distance of the support stand from the pendulum could be adjusted.

4.3 Electrical Release Mechanism

The electrical release mechanism consisted of a solenoid, a 6 volt dry cell and switch. When the current was switched on, the magnetic force from the electromagnet was strong enough to hold the pendulum at its release angle. The pendulum was released when the current was switched off. The bracket which held the solenoid could be moved along a slot to vary the release angle. This enabled a consistent method of positioning and releasing the pendulum arm.

4.4 Angular Transducer

The angular transducer was made up of two photosensors placed at 13 mm (0.5 inch) apart (See Figure 4.3). The photosensors functioned in a bright environment. When the pointer passed by the first photosensor at an arbitrary position A, the pulse triggered the counter timer (Fluke model 1953A counter-timer). When the pointer passed by the second photosensor at an arbitrary position B, the second pulse stopped the timer. The time scale on the timer ranges from 0.1 μs to 10 s. Knowing the fixed angular

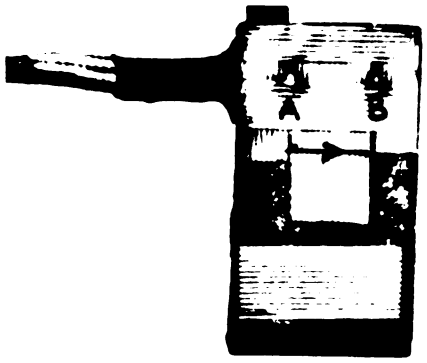

Figure 4.3 Close-up View of the Angular Transducer

distance between A and B, and the time taken to move from A to B, the angular velocity of the pointer can be calculated. To avoid interference from the shielded cable, the photosensors were placed away from the observer (Figures 4.4 and 4.5). This arrangement required an extra light source for the photosensors to perform consistently.

4.5 Force Transducer

This section will describe some strain gauge properties and temperature compensation, and Wheatstone bridge circuit before describing properties and construction of the force transducer.

4.5.1 Strain Gauge

Strain, ϵ, is a geometric property of a deformed body and is defined as extension/original length. An electrical-resistance strain gauge will change in resistance when the wire is stretched and applied strain is developed, according to the following equation:

$$\Delta R/R = G.F. \epsilon \qquad (4.1)$$

where $\Delta R/R$ is the change in resistance (ohm)/original resistance (ohm). The gauge factor (G.F.) is a property of the strain gauge (a number) and ϵ is strain (dimensionless).

Also $$E = \text{Force/Area}/\epsilon = \text{stress}/\epsilon \qquad (4.2)$$

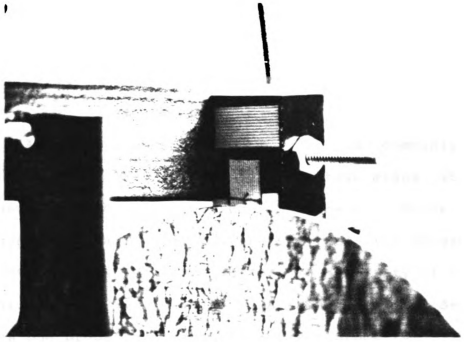

Figure 4.4 Angular Transducer Fixed Onto A Bracket

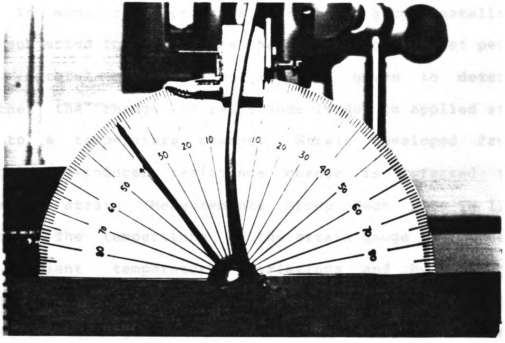

Figure 4.5 Angular Transducer Facing Away From the Observer

where E is the Young's Modulus (N/m^2) and a force (N) is applied to a cross-sectioned area (m^2). Equation 4.2 can be rewritten as:

$$\epsilon = \text{stress}/E \qquad (4.3)$$

A Wheatstone bridge circuit is commonly used to convert the $\Delta R/R$ value to a voltage signal which can be measured with a recording instrument. Since the strain gauge is small, light, precise and inexpensive, it is commonly used as the sensor in a variety of transducers (Dally and Riley, 1978). A transducer is a device which uses one property to measure another property.

4.5.2 Temperature Compensation

In many test programs, the strain gauge installation is subjected to temperature changes during the test period, and careful consideration must be given to determine whether the change in resistance is due to applied strain or to a temperature change. Strain developed from a temperature-induced resistance change is referred to as apparent strain (Measurements Group Tech Note TN 128-3, 1976). The temperature of the strain gauge is influenced by ambient temperature variations and by the power dissipated in the gauge when it is connected into the Wheatstone bridge circuit. To reduce the power dissipated in the gauge, gauge current must be minimized. Steps taken to reduce the gauge current and hence, the power

dissipation in the force transducer circuit include:

1. using 350 ohm resistance strain gauges instead of the common 240 ohm gauges,
2. employing a 5 volt instead of the 10 volt excitation voltage,
3. a temperature compensated circuit design was also used via the active full bridge circuit where the (actual strain)/(apparent strain) equals unity (Measurements Group Tech Note TN 128-3, 1976).

4.5.3 Wheatstone Bridge

The material for this section is obtained from Dally and Riley (1978). The Wheatstone bridge circuit may be used as a direct readout device where the output voltage is measured. The bridge may also be used as a null-balance system, where the output voltage is adjusted to zero by adjusting the resistive balance of the bridge.

Consider the Wheatstone bridge circuit in Figure 4.6 where the excitation voltage is E volts. The voltage drop across R_1 is denoted as V_{AB} and is given as

$$V_{AB} = E * R_1/(R_1 + R_2) \quad \text{volts} \qquad (4.4)$$

Similarly, the voltage drop across R_4 is denoted as V_{AD} and is given by

$$V_{AD} = E * R_4/(R_3 + R_4) \quad \text{volts} \qquad (4.5)$$

The output from the bridge is V_{BD} and

$$V_{BD} = V_{AB} - V_{AD} \quad \text{volts} \qquad (4.6)$$

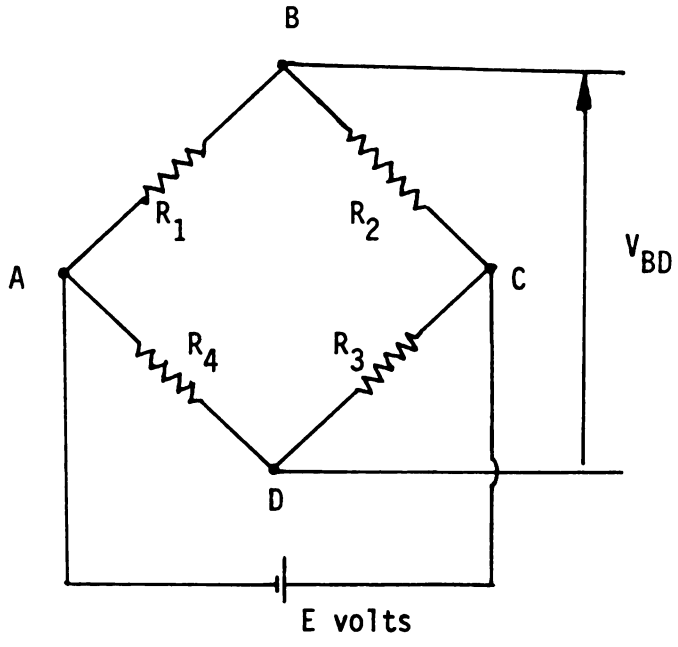

Figure 4.6 Wheatstone Bridge Circuit With E Excitation Voltage

Substituting Equations 4.4 and 4.5 into Equation 4.6 and simplification yields

$$V_{BD} = \frac{R_1 R_3 - R_2 R_4}{(R_1 + R_2)(R_3 + R_4)} E \quad \text{volts}$$

V_{BD} will go to zero and the bridge will be considered in balance when

$$R_1 R_3 = R_2 R_4$$

The bridge is initially in balance before strains are applied to the gauges in the bridge, thus the output voltage is initially at zero and the strain induced ΔV can be measured directly for both static and dynamic applications.

Since the force is linearly related to strain (Equation 4.3), as long as the ring remains elastic, the force transducer can be calibrated (See Section 5.1) so that the output signal is interpreted as a force reading. Aluminium was chosen because it has a low elasticity modulus and it is a good heat dissipator. Four 350 ohm strain gauges made for aluminium applications, model EA-13-125AC-350, were glued onto the ring with M-bond 200 adhesive (Figure 4.7A) and covered with silicon rubber for protection from the environment. These gauges were connected in an active full bridge circuit with 5 volt excitation voltage (Figure 4.7B). The letters A, B, C and D were the corresponding pin connections on the shielded cable which connected the gauges to the signal conditioner.

The signal conditioner is a black box with a high

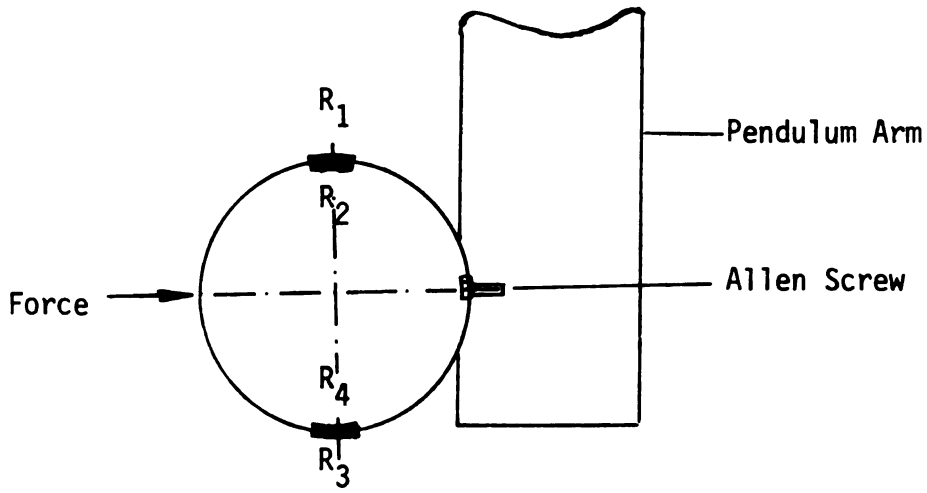

Figure 4.7A Location of Strain Gauges on the Ring

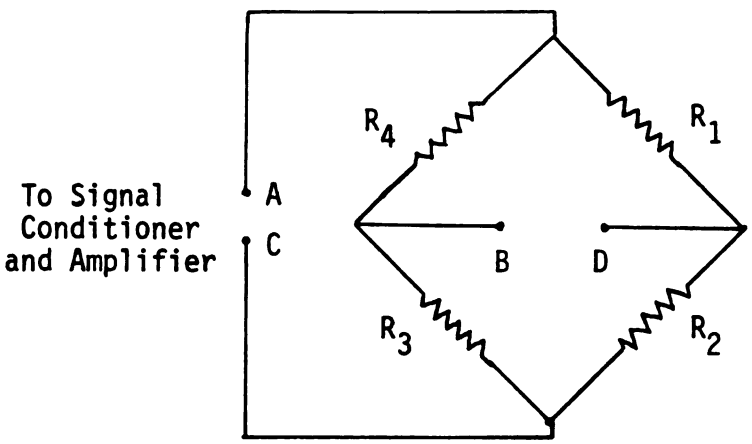

Figure 4.7B Sketch of the Force Transducer Showing the Location of the Strain Gauges and Its Circuit

input impedance (2 MΩ). It is used for balancing a Wheatstone circuit (1/4, 1/2 or full bridge) and to supply a well regulated 5 or 10 volt excitation voltage to the Wheatstone circuit. It also has a built-in voltmeter for measuring the bridge output voltage.

The power dissipation from each strain gauge is 1.14 W/in^2 . This is far below the 5 W/in^2 high precision rating for static and dynamic loading (Measurements Group Tech Note TN-502, 1979). Hence, thermal effects can be considered to be negligible. In an active bridge such as in Figure 4.7B, temperature-induced resistance change in opposite pairs is cancelled out when the strain from the inside gauges is combined with the strain from the outside gauges. The important features of this circuit were

i. it was inherently temperature compensated, hence,
ii. true strains were equal to apparent strains,
iii. effects were additive, resulting in a larger output.

The output from the signal conditioner was put into a Tektronik 59 storage oscilloscope. The storage oscilloscope provides clear visual displays of the output, with a sweep rate ranging from 0.5 μs to 5 s per division. The display on the scope can be photographed with the special equipment camera which uses a high speed polaroid film (Type 47,speed 3000).

CHAPTER V

EXPERIMENTAL PROCEDURE

This chapter is divided into two parts. The first part deals with the calibration techniques for the force transducer and the angular transducer. The latter part deals with impacting bean pods, the data collection procedures and the calculations involved to obtain impulse, maximum impact force and the energy absorbed to shatter the bean pod.

5.1 Force Transducer

A 0.6 cm (1/4 inch) diameter shielded cable was placed along the center line of the pendulum which had dimensions of 27x3x0.9 cm. The cable was used to protect the strain gauge signals from stray voltage in the environment. Therefore, the cable had to be placed as close possible to the gauges. The size and inflexibility of the cable called for a careful method of taking the cable from the pendulum to the signal conditioner without affecting the motion of the pendulum. Different ways of taking the shielded cable, perpendicularly, vertically and parallel, from the pendulum were tried (See Figure 5.1). The most suitable cable

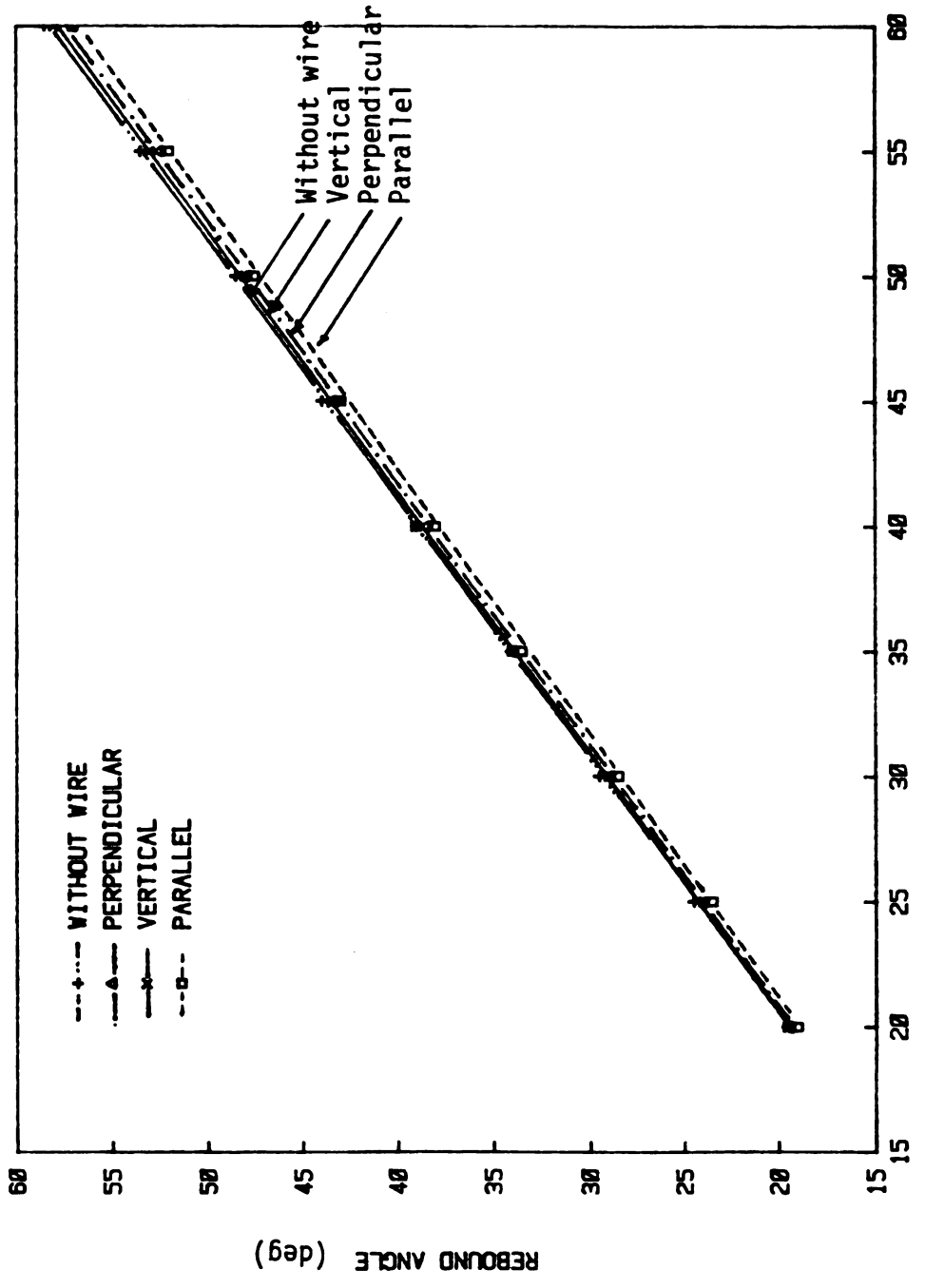

Figure 5.1 Various Ways of Taking the Shielded Cable From the Pendulum

arrangement yielded free swing rebound angles similar to those of a pendulum without the shielded cable.

A photodiode, consisting of an infrared emitter and detector embedded in a U shaped resin fixture and connected to a black box, was made to measure the maximum free swing rebound angle. The photodiode was attached to a bracket which was placed near the angle plate. The bracket was made such that it could be moved along the circumference of the angle plate. When the pendulum pointer blocked the light path from the emitter to the detector, the green light on the black box would light up. The pendulum was released at a given angle δ, if the green light on the black box did not light up, the photodiode was moved by 0.5 degree, and the pendulum was again released at δ. This procedure was repeated several times until there was green light, and the corresponding rebound angle was recorded. Each point in Figure 5.1 is an average of 3 readings. The results in Figure 5.1 suggest that taking the cable vertically was the most suitable method.

The bridge was checked for balance with a strain indicator. A balanced bridge indicates that proper solder and gauge installations were made. To ensure reliability and sensitivity, the force transducer was first connected to the signal conditioner for 70 hours to check for any drifts, then it was put under 12 continuous cycles of loading and unloading using weights and a loading platform

(See Figure 5.2). The force transducer was loaded up to 10.7 N with 0.4 N increments (up to 2.4 lb with 0.1 lb increments). The signal conditioner was connected to a Hewlett-Packett (HP) 85 computer and a 3497A data acquisition unit (See Figure 5.3).

The calibration equations obtained were:

Loading: $Y = 0.4995 + 0.665 X$; $r = 0.999$

Unloading: $Y = 0.6060 + 0.662 X$; $r = 1.000$

Average: $Y = 0.5552 + 0.663 X$; $r = 0.999$

where Y refers to the output voltage in volts and X refers to the load in newtons. To determine an average calibration value, a single curve was obtained by combining the loading and unloading conditions because both the loading and unloading curves have similar slopes (See Figure 5.4). The sensitivity of the force transducer was 1.51 N/volt (.34 lb/volt). This means that if the output voltage from the circuit is 1 volt, then the corresponding load the force transducer registers is 1.51 N.

The HP 85 computer was also used to check the impact duration with the set up shown in Figure 5.3. The pendulum was released at 40 degrees. The smallest time interval for the data acquisition unit is 1 ms. In Figure 5.5 the impact duration is 2 ms and the impulse curve is made up of only 3 data points. Even though a triangular wave can be thought of as a rough approximation of a sine wave, digitally characterizing a triangular wave requires a

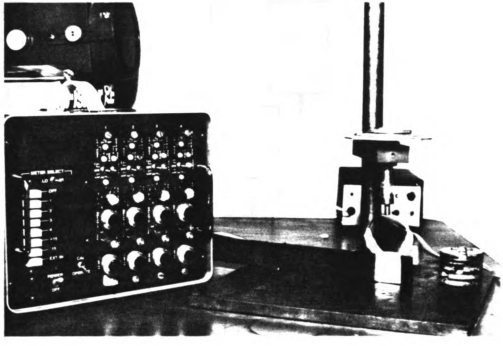

Figure 5.2 Calibrating the Force Transducer Using A Loading Platform and Standard Weights

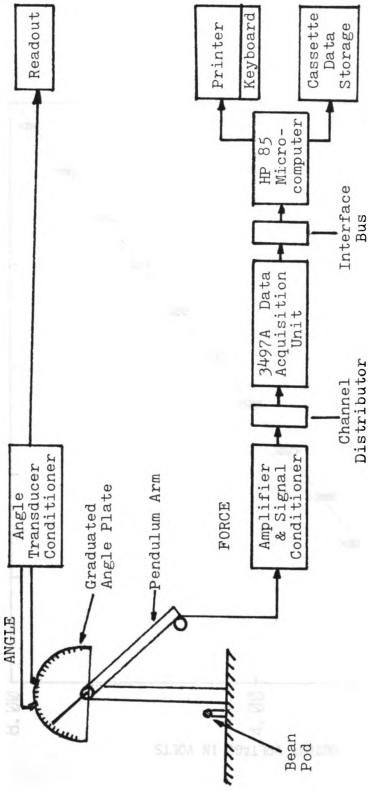

Figure 5.3 Block Diagram of the HP-85 System for Impacting Navy Bean Pods

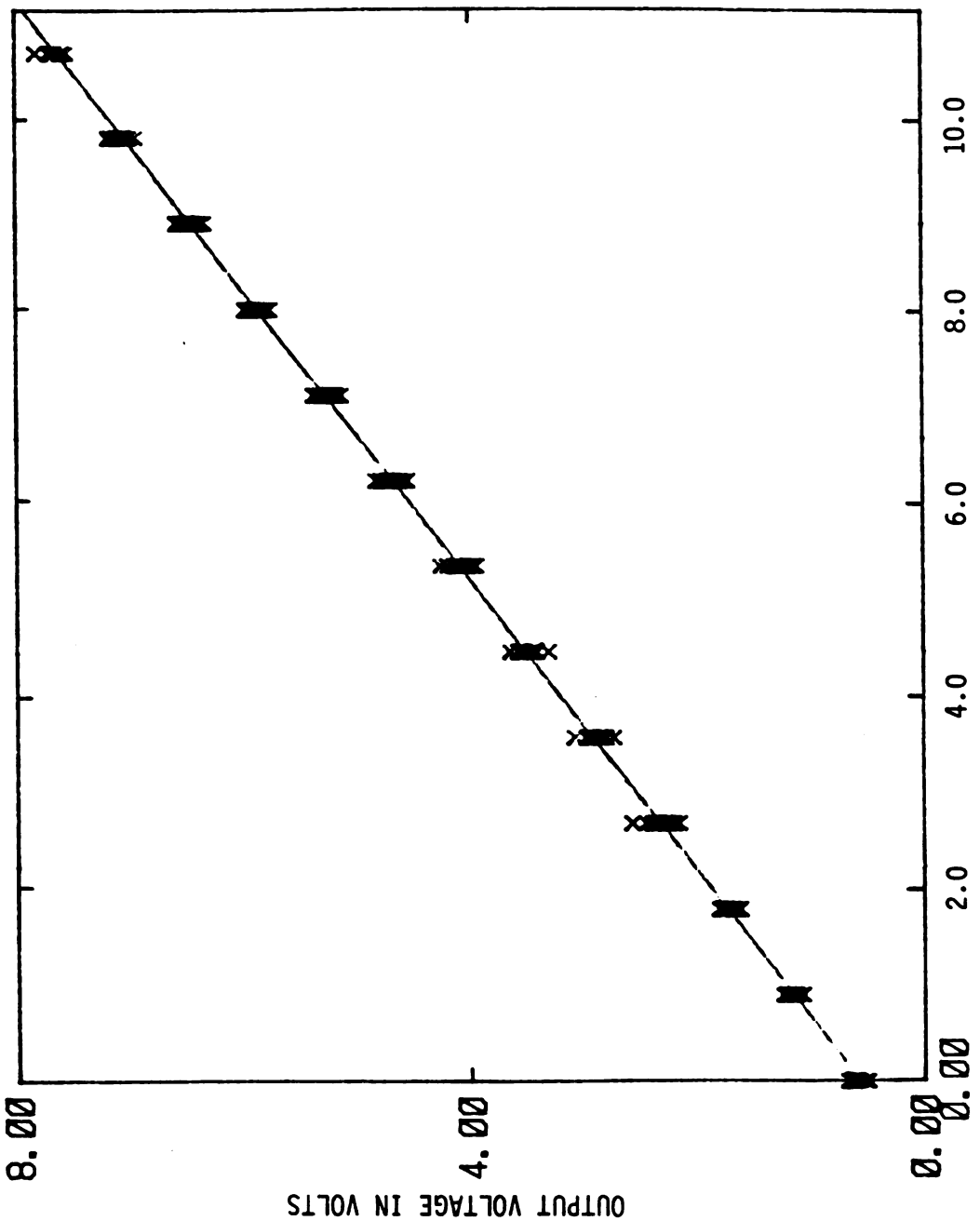

Figure 5.4 Average Calibration Curve for the Force Transducer Using Standard Weights

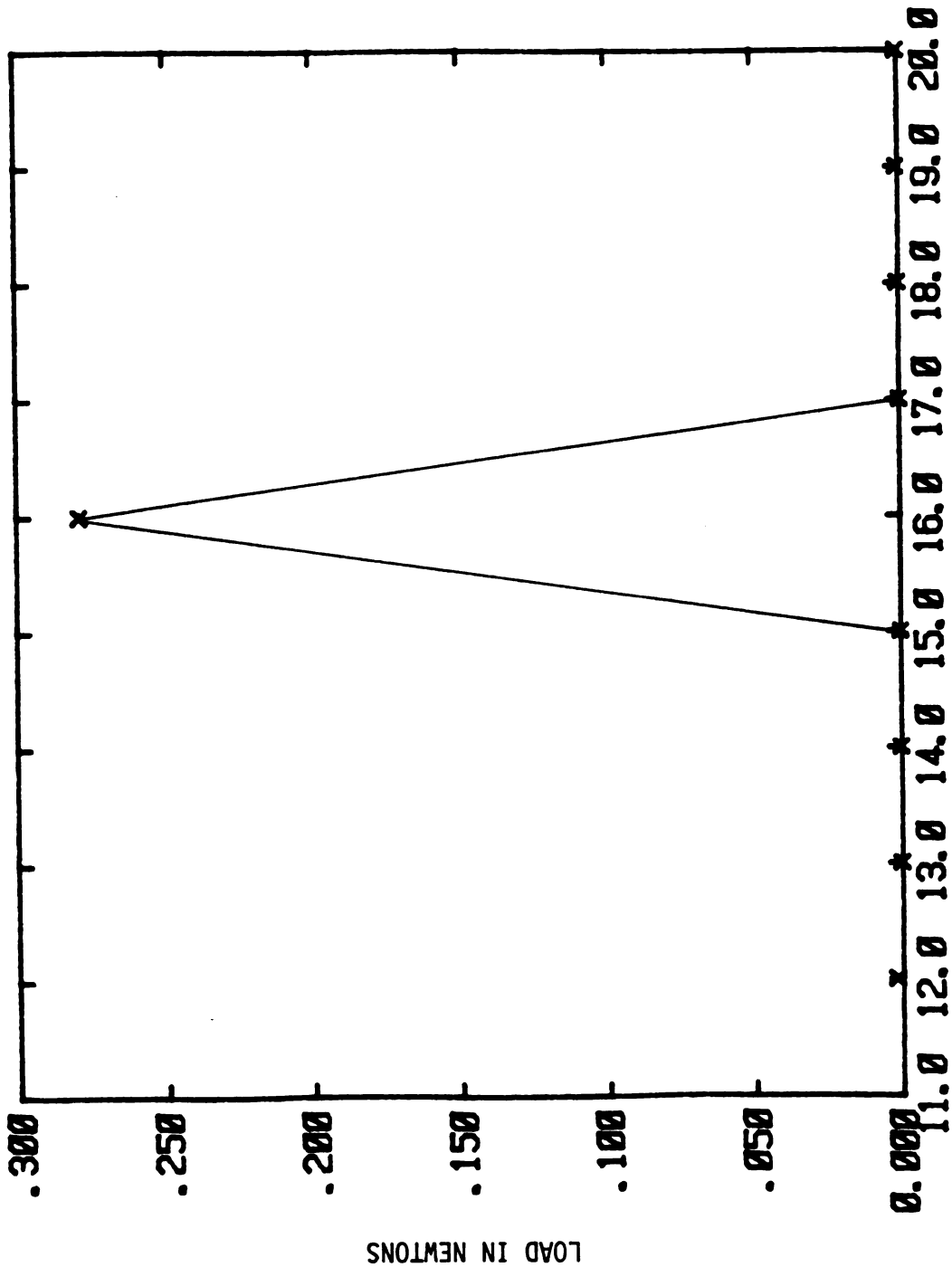

Figure 5.5 Force-Time Output From the HP-85 System

minimum of 5 points taken at equal time intervals (Affeldt, 1984). A more serious problem of having fewer data points than required creates an uncertainty whether the true peak value is recorded or not. The 3497A data acquisition unit has the smallest sampling time available for the HP system. Replacing the 3497A unit with a digital oscilloscope is not economically feasible. Nevertheless, this system gave an indication that the impact time duration was about 2 ms. This was consistent with Hoag (1972) and Srivastava et al. (1976).

A storage oscilloscope was chosen as the alternative recording instrument. According to Dally and Riley (1978), the storage oscilloscope is an ideal voltage measuring device for dynamic applications because it gives an analog output of the voltage-time plot with a wide range of time interval (1 s - 2 μs). The oscilloscope has a high input impedance (order of 1 MΩ) which means that there is no appreciable interaction between the oscilloscope and the strain gauges. The display time for the non-repetitive waveform is at the operator's discretion (0.5 s to several hours). This allows considerable time to take pictures and traces of the output.

5.2 Angular Transducer

High speed photography (Super 8 movie at 32 frames per second) was used to check the performance of the angular

transducer. The angular transducer was placed in the same bracket which held the photodiode, and fixed at 5 degrees from the vertical (See Figures 4.4 and 4.5). The pendulum was released at 40, 50 and 60 degrees for both free swings and impacting swings (with bean pods). The corresponding output on the counter-timer was also recorded. To determine the angular speed from the movies, the number of frames (f) required for the pendulum to move through θ degrees had to be counted with the aid of a film editer. By converting the θ degrees to radians, and dividing the value with (f/32) s, the angular velocity in rad/s is thus obtained. The distance between the two photosensors on the angular transducer is 5 degrees. Knowing the time from the counter-timer, the angular speed can be determined. Table 5.1 shows the results from both photography and transducer methods and each point on the graph in Figure 5.6 is an average of at least three readings.

5.3 Air Resistance

According to Mohsenin (1978), the net resistance force for most agricultural products can be given in terms of an overall drag coefficient as follows:

$$F = 1/2\ C\ Ap\ \rho\ V \qquad (5.1)$$

where

F - resistance drag force (N),

C - overall drag coefficient (dimensionless),

Table 5.1 Determination of Angular Speed Using Photography (32 frames/s) and Angular Transducer

	Average Angular Speed (rad/s)			
	Free Swing		Impacting Swing	
Release angle	Movie	Transducer	Movie	Transducer
35	3.35	3.97	2.30	2.39
40	4.46	4.47	3.35	2.97
45	4.89	5.04	3.63	3.84
50	5.50	5.59	4.42	4.77
55	5.97	6.02	4.53	4.97
60	6.61	6.58	5.59	5.79

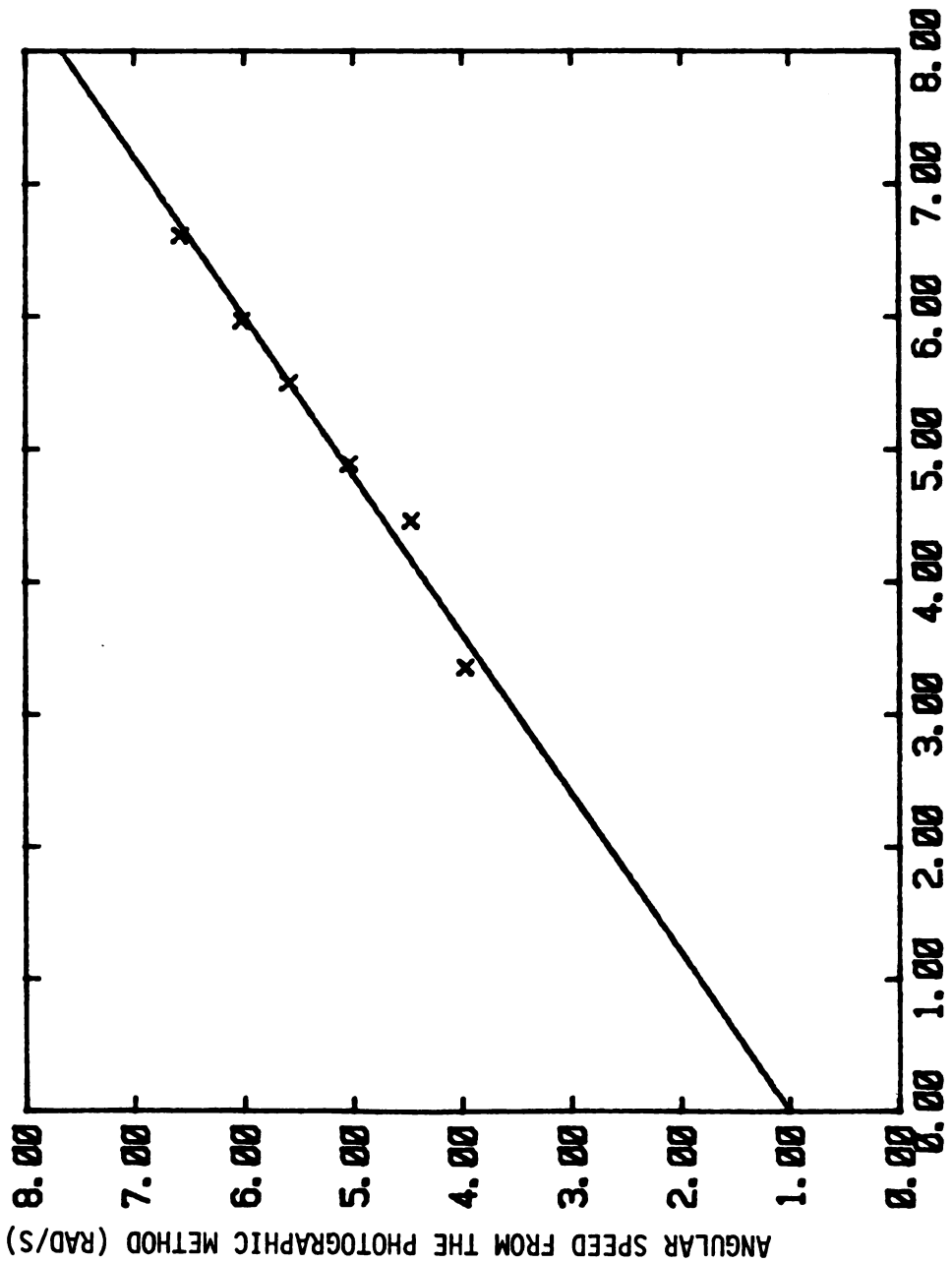

Figure 5.6 Comparisons Between the Photographic and Angular Transducer Methods

Ap - projected area normal to the direction of motion (m^2),

ρ - mass density of fluid (kg/m^3),

V - relative velocity between the fluid and the body (m/s).

The resistance force can be resolved into frictional drag due to tangential forces on the body and into profile drag due to pressure distribution around the body. In laminar flow or low velocity flow, as for the pendulum, the profile or pressure drag is negligible. The frictional drag coefficient C for a flat plate with a boundary layer is:

$$C = 1.328/ (Nr)^{0.5} \qquad (5.2)$$

where the Reynolds number Nr is defined as :

$$Nr = V \rho d / \mu \qquad (5.3)$$

where d is the effective dimension of the object, and μ is the absolute viscosity (kg/m-s). The fluid properties of air at 300K (80°F) under 1 atmosphere are as follows:

$\mu = 1.983 \times 10^{5}$ kg/m-s

$\rho = 1.1774$ kg/m^3.

The velocity V for the pendulum is computed as :

V = angular speed x pendulum length

= 5 rad/s x 0.2715 m at 45 release angle,

and d = 0.2715 m

Substitution of the above values into Equation 5.3 yields

$Nr = (5 \times .2715 \times 1.1774 \times .2715)/(1.983 \times 10^{5})$

$Nr = 218.8$

Then $C = (1.328)/ 218.8^{0.5}$

$= 0.0898$

Substituting the above values into Equation 5.1 gives:

$F = 1/2\ C\ (.009x.2715)x(1.1774)x(5x.2715)$

$F = 0.0002\ N$

Because of the small frictional force, we may assume air resistance to be negligible. Mohsenin (1978) also stated that when a plate or circular disk is placed normal to the flow, as is the case for the pendulum, the total drag will contain negligible frictional drag and it does not change with the Reynolds number. If C is approximately zero, then from Equation 5.1, the resistance force F is also zero.

5.4 Data Collection

5.4.1 Beans

Swan Valley and C-20 varieties were collected from Michigan State University farm at Swan Creek, Michigan in October, 1983. The 1984 samples were collected in October, 1984 from the university farms at College road, East Lansing. To conserve the pod moisture content, the bean pods were sealed in two layers of plastic bags and stored in a refrigerator at 4.5°C (40°F).

5.4.2 Pod Impaction

Before testing, all equipment was checked for proper working conditions. The excitation voltage was turned to zero to check for any stray voltage conditions. The shielded cable was moved and checked for proper connections. The output on the oscilloscope was checked with a 12 volt dry cell. The angular transducer was also checked for consistent performance.

Prior to testing about 400 bean pods of equal lengths, size and shape were sorted out in the refrigerator and stored again in the two layers of plastic bags. Before testing, a bag of navy bean pods of the same variety was taken out of the refrigerator and left to equilibrate with the room temperature for 10 minutes, with the bag sealed. One pod at a time was taken from the bag for testing, the bag was resealed each time after it was opened.

Bean pods of the same variety were hit at the center seeds at the three pod orientations (See Figure 5.7) following the sequence of side, top and bottom, and at release angles of 40, then 50 and finally 60 degrees. Table 5.2 illustrates the experimental layout for a single year where there are 2 replicates in each year. At these release angles all bean pods shattered at impact. A total of 10 pods were shattered for each treatment combination. A particular treatment combination has a unique combination of one release angle and one pod orientation for a

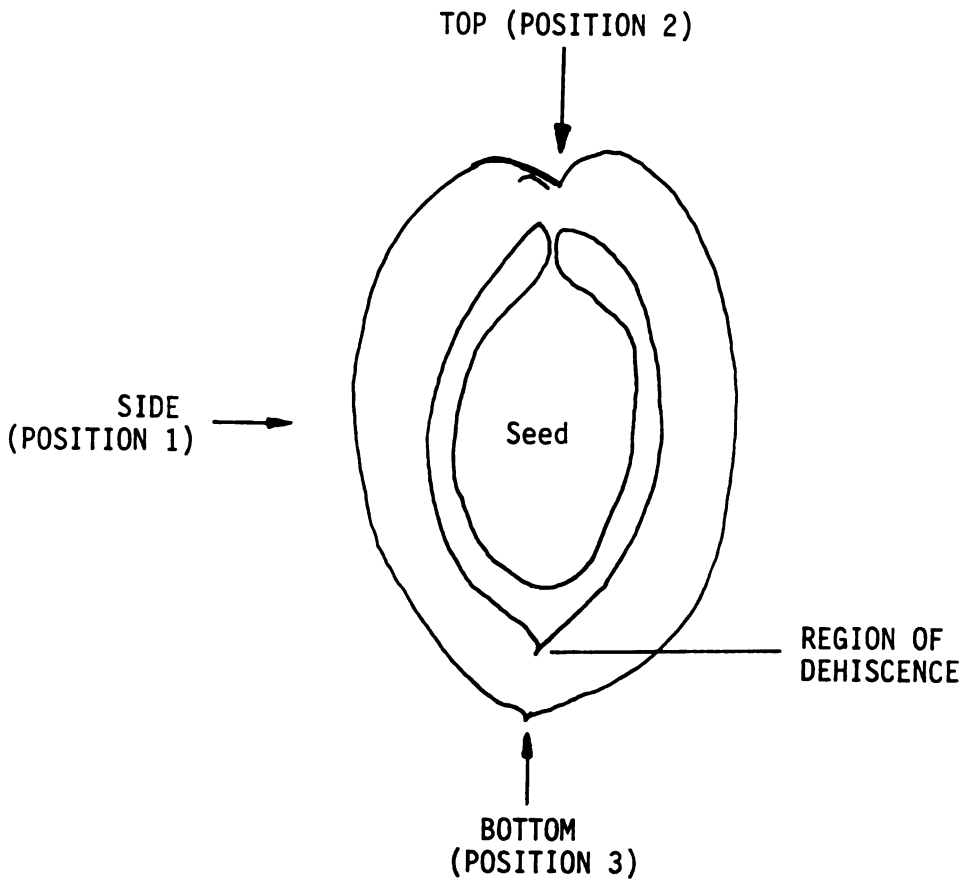

Figure 5.7 Coding of the Bean Pod Positions

TABLE 5.2 EXPERIMENTAL LAYOUT FOR A SINGLE YEAR

	Variety																	
	C-20									Swan Valley								
Release Angle	40			50			60			40			50			60		
Pod Position	S	T	B	S	T	B	S	T	B	S	T	B	S	T	B	S	T	B
No. Day 1	10	10	10	10	10	10	10	10	10	10	10	10	10	10	10	10	10	10
No. Day 2	10	10	10	10	10	10	10	10	10	10	10	10	10	10	10	10	10	10

Note: S means side
T means top
B means bottom

particular variety. All 18 treatment combinations for both varieties were performed on the same afternoon. The same experiment was repeated 2 days later for replication. A total of 720 pods were shattered, pods which did not shatter (3 pods) were not recorded, so as to facilitate computation of impulse, maximum impact force and the absorbed energy to shatter. The output on the oscilloscope was traced with permanent ink on transparent plastic which had 1 cm grid lines on it. This gave a fast and economical method to trace results compared to the polaroid film which needed 10 minutes to develop the film. Pictures of some impact traces were taken with the poloroid as well as traced on plastic for verification.

Typical outputs on the poloroid and plastic grid are shown in Figure 5.8. The impulse curve is not symmetrical, which is typical for agricultural products where elastic-plastic deformations are common (Mohsenin, 1978). The ripples on the down slope are probably due to the sequence of pod deformation and failure followed by further deformation and failure until the pod finally shatters and the output voltage goes to zero. For comparison purposes, an output from an undeformed cylindrical material has a smooth down slope curve (See Figure 5.9). The movies do not show the shatter sequence because the time between successive frames is 0.03 s which is far bigger than the 0.5 ms/cm horizontal scale on the volt-time curve.

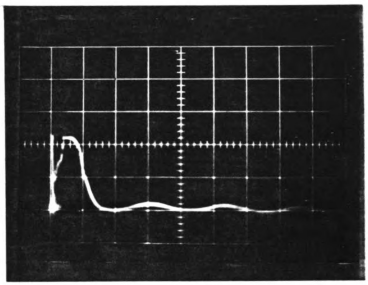

(A)

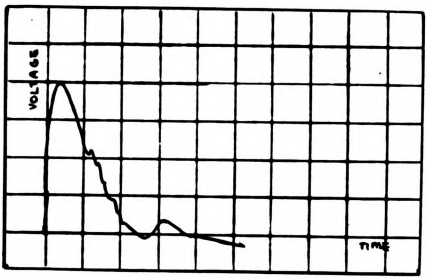

(B)

Figure 5.8 Typical Output on the (A) Poloroid and (B) Plastic Grid

The bean pods and seeds were then dried in a forced air oven at 103 C for 24 hours. This procedure was done by Hoag (1972), Weeks, Wolford and Kleis (1975), and Hummel and Nave (1976). Preliminary tests justified the 24 hours of drying time since only a small difference in mass (0.5 percent) existed after another 48 hours of continuous drying, making it a total of 72 hours. Table 5.3 shows the moisture content of bean pods together with seeds, wet basis, for each sample.

The valves of the navy bean pod twist the pod as it is broken, thereby expelling the seeds. This feature is characteristic for architype navy beans. Figure 5.10 shows a picture of twisted navy bean pods which shattered after impact.

5.5 Computation of Calculated Values

This section describes the computation for impulse, maximum peak force and energy absorbed to shatter. The computation for all data sets was done with the SPSS computer program (See Section 6.1).

5.5.1 Impulse

Impulse is defined as the value under the force-time curve (Equation 3.12), which was obtained from the oscilloscope. The area under the curve was determined by counting the number of square cm using the grid lines and

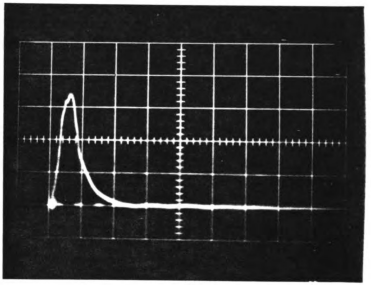

Figure 5.9 Output From An Undeformed Cylindrical Material

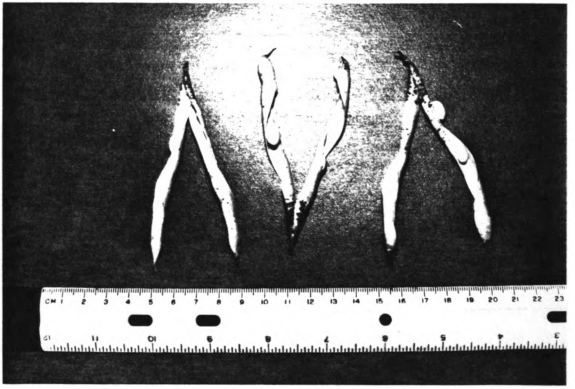

Figure 5.10 Twisted Navy Bean Pods After Shatter

Table 5.3 Moisture Content For Both Bean Pod and Seeds (wet basis) For All Samples

Year	Variety	Replicate	m.c.%(wb)
1983	C-20	1	13.34
1983	C-20	2	13.40
1984	C-20	1	14.09
1984	C-20	2	14.21
1983	Swan Valley	1	13.60
1984	Swan Valley	2	13.84
1984	Swan Valley	1	14.75
1984	Swan Valley	2	15.15

graph paper with 1 mm grids placed under the plastic. The vertical scale for the output voltage was 5 volt/cm and the horizontal scale was 1 ms/cm, and recalling that the force transducer calibration was 1.51 N/volt, gives

$$1.51 \text{ N/volt} * 5 \text{ volt/cm} * 1 \text{ ms/cm} = 7.54 \text{ N-ms/cm}^2$$

This factor was multiplied with the area under the volt-time curve (in cm^2) for computation of impulse (N-ms) in the SPSS program.

5.5.2 Maximum Impact Force

Similarly, the vertical scale on for the output voltage was 5 volt/cm and the calibration for the force transducer was 1.51 N/volt. Multiplying the two values yield 7.55 N/cm. This factor was multiplied with the maximum voltage (in cm) on the volt-time curve in the SPSS program to give the corresponding maximum impact force in newtons.

5.5.3 Energy Absorbed

Before the value of the absorbed energy can be computed, the value of the pendulum moment of inertia must be calculated first. The compound pendulum consisted of a steel bar, an aluminium ring and shielded cable. These individual components contribute to the calculation of pendulum moment of inertia. The moment of inertia for the compound pendulum was 0.002 $kg\text{-}m^2$. Using Equation 3.8, a

general equation for the computation of absorbed energy was obtained by multiplying all the constants in the equation to give:

$$Ep = 0.00725[(1/T_1^2) - (1/T_2^2)] \text{ mJ}$$

where T_1 and T_2 refer to the times before and after impact, as recorded on the counter-timer. The values of T_1 and T_2 were the input values into the SPSS program to compute the values of absorbed energy in mJ.

5.6 Accuracy of Measurements

The size of the ring was chosen empirically. Compression tests on 3 cm, 4 cm and 5 cm (1.19, 1.75, 2 inches) diameter rings using the Instron machine at 0.2 cm/s (5 inches/min) were used to select the ring diameter which had the maximum deformation under a given load. The 5 cm (2 inch) diameter ring was selected as the most suitable size. Calibration for the ring was done statistically (See Section 5.1 and Figure 5.4). The variance of the output voltage s_{qo}^2 can be obtained using the following equation from Doebelin (1975):

$$s_{qo}^2 = 1/N \Sigma (mq_i + b - q_o)^2 \qquad (5.4)$$

where N - total number of data points

m - gradient of the calibration curve (volt/N)

b - intercept on the vertical axis of the calibration curve

q_i - input value (force in newtons)

q_o - output value (volts)

From Figure 5.4 N = 300

m = 0.6627 (volt/N)

b = 0.1248

for pairs of q_o and q_i yields

$s^2_{qo} = 0.01423$

and $s^2_{qi} = s^2_{qo}/m^2 = 0.0324$

then $2s_{qi} = 0.18$

The input value can be described by:

$$q_i = (q_o - b)/m \qquad (5.5)$$

If the static output voltage is 4.0 volts, then the corresponding force is 5.20 ± 0.18 N with a probability of 95 percent. The error term is ± 3 percent.

The value on the volt-time curve can be read to the nearest ± 0.1 cm on both axes. This gives the voltage error of ±0.25 volt on a 5V/cm scale. The output variance for dynamic calibration is $s^2_{qody} = (0.25/2)$. The total ouput variance is

$$s^2_{qout} = s^2_{static} + s^2_{dynamic} \qquad (5.6)$$

$$= 0.0324 + 0.0156$$

$$= 0.048$$

Then the error term for the output voltage is $\pm 2s_{qout}$ which is ± 0.44 N. The error in reading the vertical and horizontal axes of the volt-time curve is ± 0.1 cm. Given a mean value of 3 cm for the peak voltage gives an error of ± 0.3 cm, and a mean value of 2 cm for the duration of

impact on the horizontal axis gives an error value of ± 0.2 cm. The error in calculating the area under the volt-time curve is

$$\pm (0.03 + 0.02)\ cm^2 = \pm 0.05\ cm^2$$

If the area under the volt-time curve is 3 cm^2, then the corresponding impulse value is 22.62 ± 0.38 N-ms or ± 2 percent error.

The response time of the photosensors is in the order of nanoseconds (10^{-9} s). The counter-timer could read a time range of 0.1 μs to 10s. The counter has an accuracy of ± 1 count which means that the error in measuring the time interval between the photosensors is ± 0.0001 s. The response time of the photosensors is 100 times faster than that of the counter-timer, we may assume that the error for calculating the time interval to depend on the accuracy of the counter-timer. Given that the angular distance between the photosensors is 5 ± 0.5 degrees, a T_1 value of 0.0195 s and a T_2 value of 0.0250 s, then the corresponding absorbed energy value is 7.47 ± 0.06 mJ or ± 1.0 percent.

The output curves in Figure 5.8 suggest that the force transducer is a second order instrument. The general equation to describe the output is as follows:

$$a_2\frac{dq_0}{dt^0} + a_1\frac{dq_0}{dt^0} + a_0 q_0 = b_0 q_i$$

$K = b_0/a_0$ is the static calibration

The general equation to describe the impulse response of a second order instrument is :

$$\frac{q_0}{KA\omega_n} = \frac{1}{\sqrt{1-\zeta^2}} e^{-\zeta\omega_n t} \sin(\sqrt{1-\zeta^2}\,\omega_n t) \qquad (5.7)$$

where A^* - area under the impulse curve

ω_n - natural frequency of the transducer (rad/s)

ζ - damping ratio

t - time

The values of ω_n and ζ are computed using the equations

$$\omega_n = 2\pi / (T - \sqrt{1-\zeta^2}) \qquad (5.8)$$

$$\zeta \simeq [\log (x_1/x_n)]/2\pi n \qquad (5.9)$$

where T is the period of the oscillations

x_1 and x_n are successive n peaks on the output graph. The values of ω_n = 3320 rad/s and ζ = 0.023 are computed from Figure 5.8. To maximize the output Equation 5.7 is differentiated with respect to time which yields a value of t = 0.00047, substituting this value into Equation 5.7 yields

$$q_0/KA\,\omega_n = \sin(88.7) \simeq 1.0$$

which is expected of a second order instrument.

The accuracy of the force transducer and the angular transducer were not determined from application of equations. Rather, the error term for the force transducer was determined statistically from the calibration results and that for the angular transducer was determined empirically. The error term for the force transducer is ± 3 percent which means that when the output voltage is 16.0 volts, then the corresponding force is 20.80 ± 0.44 newtons

with a probability of 95 percent. When the area under the volt-time curve is 3 cm^2, then the corresponding impulse value is 22.62 $\pm$ 0.38 N-ms or $\pm$ 2 percent error. When the times before and after impact are 0.0195 and 0.0250 s, then the corresponding absorbed energy value is 7.47 $\pm$ 0.06 mJ or $\pm$ 1 percent error.

CHAPTER VI

RESULTS AND DISCUSSIONS

Computation of energy absorbed by the bean pod, maximum impact force and impulse for all the 720 sets of data and the statistical analysis were incorporated into the SPSS (Statistical Package for Social Sciences) on the mainframe Cyber Computer at the Computer Center, M.S.U. The computational procedures are described in Section 5.6.

Before using the program, the experimental factors were coded as follows:

Year	(1)	1983	(2)	1984		
Variety	(1)	C-20	(2)	Swan Valley		
Release Angle	(1)	40	(2)	50	(3)	60
Pod Position	(1)	Side	(2)	Top	(3)	Bottom

The input data from experimental measurements were: area under the volt-time curve (cm^2), maximum voltage on the volt-time curve (cm), times before and after impact, T_1 and T_2 in seconds as recorded on the counter-timer and the corresponding replicate number, that is, replicate 1 for day 1 and replicate 2 for day 2. Figure 6.1 shows the computation and coding for the program.

```
*  RUN NAME       NAVYBEANS ANALYSIS
*  FILE NAME      NAVYBEANS
*  VARIABLE LIST ID,SET,YEAR,VAR,ANGLE,POS,VOL,AREA,T2,T1,REP
*  INPUT FORMAT  FIXED(F3.0,F3.0,F2.0,F2.0,F2.0,F2.0,F3.1,F3.1,F4.4,F4.4,F2.0)


   ACCORDING TO YOUR INPUT FORMAT, VARIABLES ARE TO BE READ AS FOLLOWS

   VARIABLE    FORMAT   RECORD      COLUMNS

   ID          F 3. 0        1       1 -  3
   SET         F 3. 0        1       4 -  6
   YEAR        F 2. 0        1       7 -  8
   VAR         F 2. 0        1       9 - 10
   ANGLE       F 2. 0        1      11 - 12
   POS         F 2. 0        1      13 - 14
   VOL         F 3. 1        1      15 - 17
   AREA        F 3. 1        1      18 - 20
   T2          F 4. 4        1      21 - 24
   T1          F 4. 4        1      25 - 28
   REP         F 2. 0        1      29 - 30

THE INPUT FORMAT PROVIDES FOR 11 VARIABLES.    11 WILL BE READ.
IT PROVIDES FOR 1 RECORDS  (*CARDS*)  PER CASE.
A MAXIMUM OF   30  *COLUMNS*  ARE USED ON A RECORD.

*   N OF CASES        720
*   VAR LABELS        VAR  VARIETY/
*                     POS  POSITION/
*                     VOL  VOLTAGE/
*                     AREA  AREA UNDER CURVE/
*                     T1   FREE SWING TIME/
*                     T2   IMPACT SWING TIME
*   VALUE LABELS      YEAR (1)1983  (2)1984/
*                     VAR  (1)C20   (2)SWAN VALLEY/
*                     ANGLE (1)40 DEG  (2)50 DEG  (3)60 DEG/
*                     POS  (1)SIDE  (2)TOP  (3)BOTTOM
*   COMPUTE           ENERGY=0.0072546086*((1/(T1*T1))-(1/(T2*T2)))
*   COMPUTE           FORCE=7.5444369*VOL
*   COMPUTE           IMPULSE=7.5444369*AREA

*   ANOVA             ENERGY BY YEAR(1,2)VAR(1,2)ANGLE(1,3)POS(1,3)/
*                     FORCE BY YEAR(1,2)VAR(1,2)ANGLE(1,3)POS(1,3)/
*                     IMPULSE BY YEAR(1,2)VAR(1,2)ANGLE(1,3)POS(1,3)
*   STATISTICS        1
```

Figure 6.1 Coding and Computation on the SPSS Program

6.1 Results

The results for absorbed energy, maximum impact force and impulse are listed in Tables 6.1 and 6.2 for 1983 and 1984 respectively. Each value in the table is an average of the readings from 20 shattered pods. Table 6.3 gives the mean values and ranges for all of the 720 computed values.

The SPSS program is primarily used for the social sciences thus, a few modifications had to be made before an analysis of variance could be performed for biometrical applications. In this study samples were taken in 2 years and for each year, the samples were collected from different locations, namely Swan Creek and East Lansing. There is no replication of sample location but rather, a replication of year (time). Hence, a sum of squares value for replication within year is required. This is listed as "Replication (year)" in the analysis of variance tables of Tables 6.4, 6.6 and 6.9 where the degrees of freedom are obtained from the formula:

number replicate*(number year - 1)

where the number of replicates and year is 2 for this study.

There are 10 readings for each treatment combination and this requires a sampling error term and the sampling error sum of squares to be included in the analysis of variance table. The residual sum of squares obtained directly from

Table 6.1 Results For 1983

		Variety					
		C-20			Swan Valley		
Release Angle		40°	50°	60°	40°	50°	60°
Impulse	Side	35.08	24.03	21.88	29.23	29.99	27.35
(N-ms)	Top	27.99	24.03	24.37	26.78	25.05	23.35
	Bottom	21.16	22.94	17.28	20.75	20.14	19.01
Max	Side	27.73	23.43	24.14	26.10	27.52	25.92
Force	Top	27.12	24.44	25.65	26.75	27.20	25.95
(N)	Bottom	24.56	24.67	22.48	24.75	26.78	25.20
Absorbed	Side	12.95	14.42	12.00	9.22	11.84	10.99
Energy	Top	10.53	11.32	12.02	8.62	10.38	9.21
(mJ)	Bottom	8.57	12.86	10.62	7.34	10.46	7.79

Table 6.2 Results For 1984

		Variety					
		C-20			Swan Valley		
Release Angle		40°	50°	60°	40°	50°	60°
Impulse	Side	30.37	23.20	26.75	31.72	30.86	30.18
(N-ms)	Top	23.84	22.75	25.61	20.97	23.35	24.37
	Bottom	17.24	20.48	20.18	19.58	22.90	20.60
Max	Side	24.71	21.84	24.29	25.65	25.35	24.26
Force	Top	22.33	23.20	24.03	24.33	24.63	24.07
(N)	Bottom	22.03	23.35	24.23	23.46	26.22	23.99
Absorbed	Side	8.19	12.14	10.17	7.61	10.54	11.45
Energy	Top	8.32	11.29	10.68	8.22	10.81	16.94
(mJ)	Bottom	8.53	10.14	7.13	6.06	8.71	7.77

Table 6.3 Table of Means and Ranges of Computed Values for All 720 Bean Pods

	Mean	Maximum	Minimum
Impulse (N-ms)	24.32	71.67	6.04
Max Impact Force (N)	24.82	36.97	11.32
Absorbed Energy(mJ)	10.16	31.50	1.40
Duration of Impact (ms)	1.76	4.4	0.7

the SPSS program was a combination of sampling error, experimental error and replication error sum of squares all lumped into one. The SPSS program was modified to enable computation of sampling error sum of squares and replication sum of squares. The sampling error sum of squares was determined by using treatment combinations, termed as "set" in Figure 6.1,where there are a total of 72 treatment combinations, as the only variable in the SPSS program. The replication sum of squares was obtained by using replicate 1 and 2 as the only variable in another run of the program. The experimental error sum of squares was obtained by subtracting the sampling error and replication sum of squares from the residual sum of squares obtained earlier. The F value in Tables 6.4, 6.6 and 6.9 is the mean sum ofsquares/experimental sum of squares ratio.

The results and discussions will be divided separately into impulse, maximum impact force and energy absorbed to shatter.

6.2 Impulse

The analysis of variance table for impulse is shown in Table 6.4. The only significant main effect is position and none of the interactions are significant. A one-way analysis for pod position is done using the LSD (Least Significant Difference) at the 95 percent confidence level. The LSD procedure is useful for making comparisons between

Table 6.4 Analysis of Variance for Impulse

Source	df.	SS	MS	F
Rep(year)	2	711.73	355.865	1.730
Year	1	16.621	16.621	0.081 ns
Variety	1	160.796	160.796	0.782 ns
Angle	2	482.902	241.451	1.174 ns
Position	2	8066.584	4033.292	19.604 ***
Year-variety	1	69.732	69.732	0.399 ns
Year-angle	2	840.366	420.183	2.042 ns
Year-position	2	224.023	112.012	0.544 ns
Variety-angle	2	409.578	204.789	0.995 ns
Variety-position	2	440.911	220.456	1.072 ns
Angle-position	4	1067.668	266.917	1.298 ns
Year-variety - angle	2	136.619	68.309	0.332 ns
Year-variety -position	2	91.112	45.556	0.221 ns
Year-angle -position	4	36.621	9.155	0.044 ns
Variety-angle -position	4	577.034	144.258	0.701 ns
Year-variety -angle-position	4	194.263	48.566	0.236 ns
Expt. error	34	6995.124	205.739	
Sampling error	648	50112.609	77.334	
Total	719	70634.293	98.24	

Note: 1. Rep(year) - replication within year
SS - Sum of Square of deviations about a mean
df - degree of freedom
MS - Mean Square i.e. Sum of Square divided by degrees of freedom
expt.- experimental

2. $F_{0.5}(1,30) = 4.17$
$F_{0.5}(2,30) = 3.32$
$F_{0.5}(4,30) = 2.69$

two or more mean values. In this case, if the difference in impulse between pod positions is less than the LSD value, then the differences in impulse may be due to chance or minor environmental differences. If, however, the difference is greater than the LSD value, there is a 95 percent probability that their mean impulse values actually are different for different pod positions.

From Table 6.4 $s^2 = 205.739$

$$s_d^2 = 2(s^2)/240$$

$$LSD = t_{\alpha/2}\, s_d$$

$$= 2.024\sqrt{2\ (205.739)/240}$$

$$= 2.65$$

The results in Table 6.5 indicates that all the pod positions are significantly different at an LSD value of 2.65 for a two-tail t test at $\alpha = 0.05$ since all mean differences exceed the LSD value. Position 1 has the highest mean, followed by position 2 and Position 3 (Figure 6.2). This suggests that the bean pod is strongest when it is hit on the side, and weakest when it is hit along the base.

The mean impulse values for each pod position was expected to be different because the distance between the bean seed and the pericarp is different for different orientations (Figure 5.7). The thickness of the pericarp is not uniform. There is a column of thickened cells running along the length of the pod suture at the top

Table 6.5 Table of Means for Impulse With Pod Position

		Pod Position		
		Pos 1	Pos 2	Pos 3
		28.39	24.37	20.19
Pos 3	20.19	* 8.20	* 4.18	-
Pos 2	24.37	* 4.02	-	
Pos 1	28.39	-		

* significant at 95 percent.

LSD = 2.65

Pos 1	Pos 2	Pos 3
a		
	b	
		c

Underlined with same line do not have significant differences at $\alpha = 0.05$.

Mean position 1 = a

Mean position 2 = b

Mean position 3 = c

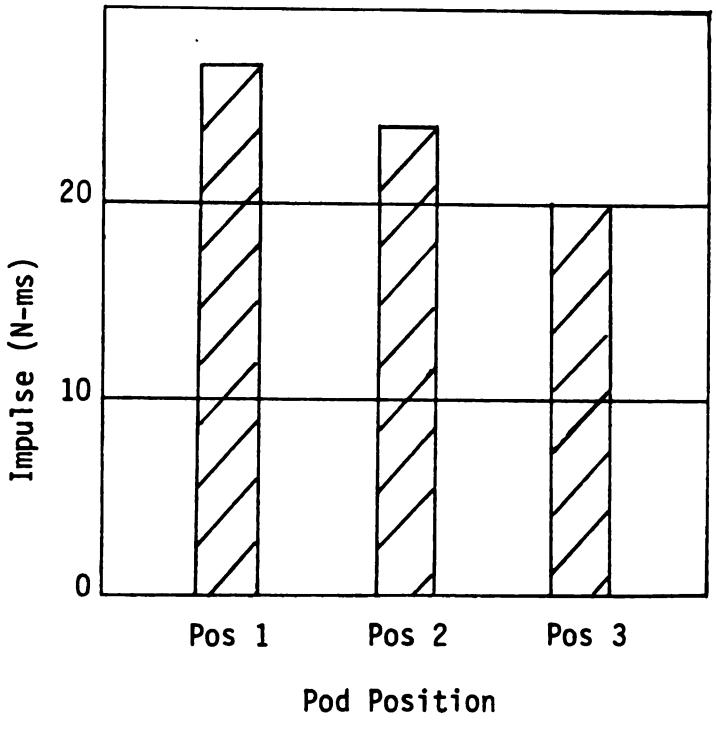

Figure 6.2 Plot of Mean Impulse For Different Pod Positions

position. The base of the pod is furthest away from the bean seed and it looks as if the space between the seed and the pericarp is cushioning some of the impacting force. When the pod is hit perpendicularly at the bottom, the shape of the pod which is similar to the shape of a keel, may offer some reinforcement by resisting deformation imposed by the impact from being transmitted to the region of dehiscence. At the region of dehiscence there is a concentration of energy which causes the pod to fail under tension and consequently causes the pod to burst and the valves to curl. At position 1 the bean seed is nearest to the pericarp but furthest away from the pod's seams and it seems to be where the pericarp is the thinnest. There is no concentration of energy at the side position and it is where the energy waves have to travel the furthest to any point where energy is concentrated or to the pod's seams. It is surprising to expect the bean pod to be strongest when hit on the side. When the pod is hit at the pod suture (top position) the impact is transmitted to the region of dehiscence which consequently causes the pod to shatter. Reported research on soybean pods has shown that the thickness of the pericarp depended on the position of the bean pods on the plant (Weeks et al., 1975). Preliminary tests showed that the bean pods break more easily when hit on the seed than when hit between the seeds. Preliminary impact tests (Figure 6.3) on 1983 Swan

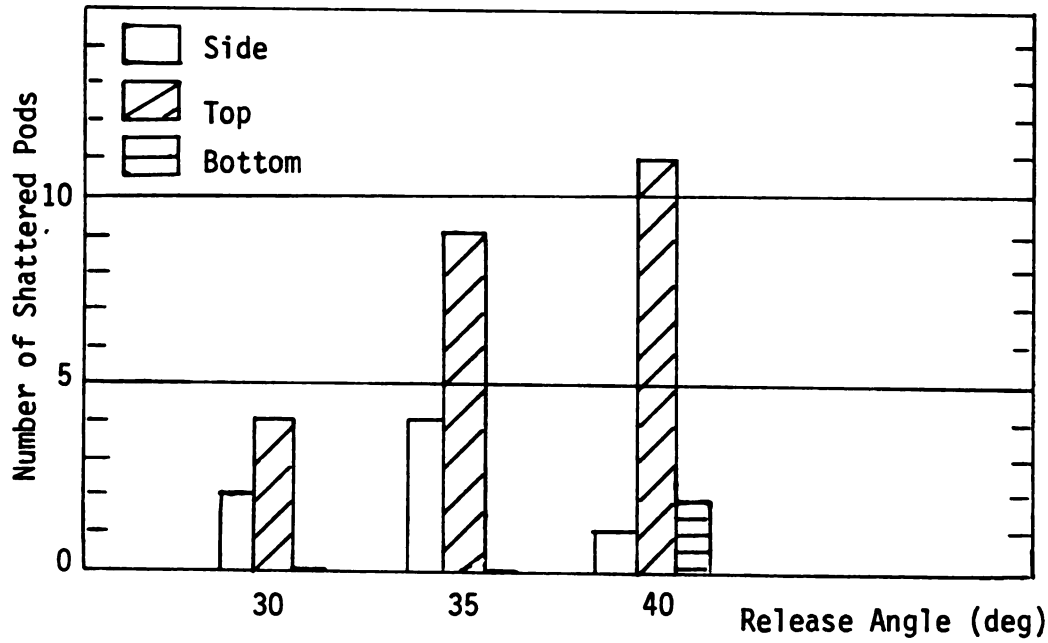

(A) Distance between supports is 7.5 cm

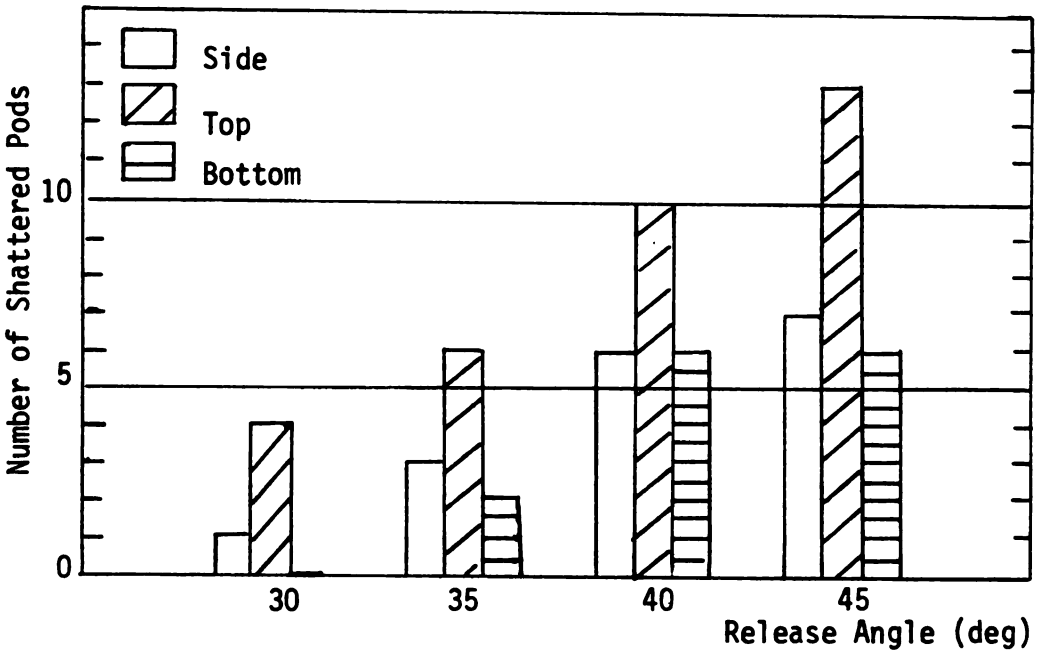

(B) Distance between supports is 6.5 cm

Figure 6.3 Plot of Number of Shattered Pods After Impact at Different Release Angles and Pod Positions for 1983 Swan Valley Pods for Two Supports Distances

Note: Number of pods in each treatment is 14

Valley bean pods in Summer 1984 suggest that the bean pod is weakest along the pod suture (Position 2) but the results do not indicate clearly whether the bean pod is strongest along the side (Position 1) or not.

6.3 Maximum Impact Force

The analysis of variance was done with year as a factor as seen in Table 6.6. Significant factors are year and variety while the significant interaction is the two-way interaction between variety and release angle. The average maximum impact force values for the two years are as follows.

1983: max force = 25.64 N

1984: max force = 24.10 N

difference = 1.54 N

From Table 6.6 $s^2 = 26.81$

$$s_d^2 = 2(26.81)/360$$

$$LSD = t_{\alpha/2}\, s_d$$

$$= 2.024(.3859)$$

$$= 0.78$$

There is a significant difference between the year means at an LSD value of 0.78 at two tail t test of $\alpha = 0.05$. The difference in the mean values is probably due to maturity characteristics of the navy bean pods. Similarly, the average maximum impact force for the two varieties are given below:

Table 6.6 Analysis of Variance for Maximum Impact Force

Source	df	SS	MS	F
Rep(year)	2	93.741	46.871	1.748 ns
Year	1	483.431	483.431	18.032 ***
Variety	1	346.447	346.447	12.922 **
Angle	2	32.587	16.294	0.608 ns
Position	2	97.389	48.695	1.816 ns
Year-variety	1	0.620	0.620	0.023 ns
Year-angle	2	84.469	42.234	1.575 ns
Year-position	2	72.933	33.467	1.248 ns
Variety-angle	2	229.839	114.919	4.286 *
Variety-position	2	12.173	6.086	0.227 ns
Angle-position	4	174.809	43.702	1.630 ns
Year-variety -angle	2	113.374	56.687	2.114 ns
Year-variety -position	2	3.274	1.637	0.061 ns
Year-angle -position	4	32.769	8.192	0.306 ns
Variety-angle -position	4	74.785	18.696	0.697 ns
Year-variety -angle-position	4	36.981	9.25	0.345 ns
Expt. error	34	911.554	26.81	
Sampling error	648	5877.749	9.071	
Total	719	8678.925	12.071	

Note: 1. Rep(year) - replication within year
SS - Sum of Squares of deviations about a mean
df - degree of freedom
MS - Mean Square i.e. Sum of Square divided by degrees of freedom
expt.- experimental

2. $F_{0.5}(1,30) = 4.17$
$F_{0.5}(2,30) = 3.32$
$F_{0.5}(4,30) = 2.69$

C-20: max force = 24.12 N

Swan Valley: max force = 25.51 N

difference = 1.39 N

Using the LSD value of 0.78 as before gives a significant difference in maximum impact force between the two varieties. The varieties have different performances for maximum impact force. The table of means for the variety-release angle interaction is shown in Table 6.7. A plot of these values are shown in Figure 6.4. At 40 and 60 degrees release angles, the maximum impact forces are about the same but at 50 degrees release angle, there is a dip in the curve for the C-20 variety but a peak for the Swan Valley variety. The average impact force for the two varieties are not similar and we expect some interactions between variety and year. The interaction between year and variety is significant but the reasons are not clear.

Generally the maximum impact force values are higher for the 1983 results than that for 1984 (See Table 6.8). The maximum impact force values for the Swan Valley variety are generally higher than C-20.

Pickett (1973) and Singh (1975) both agreed that moisture content affects threshability of navy bean pods. Hoag (1975) also found that moisture content affects the maximum force to damage soybean pods. These findings agree that the difference in moisture level contributes variability in the mean maximum impact force to initiate

Table 6.7 Table of Means for Interaction Between Release Angle and Variety for Maximum Impact Force.

	Variety	
	C-20	Swan Valley
Release Angle		
40	24.75	25.17
50	23.45	26.46
60	24.14	24.90

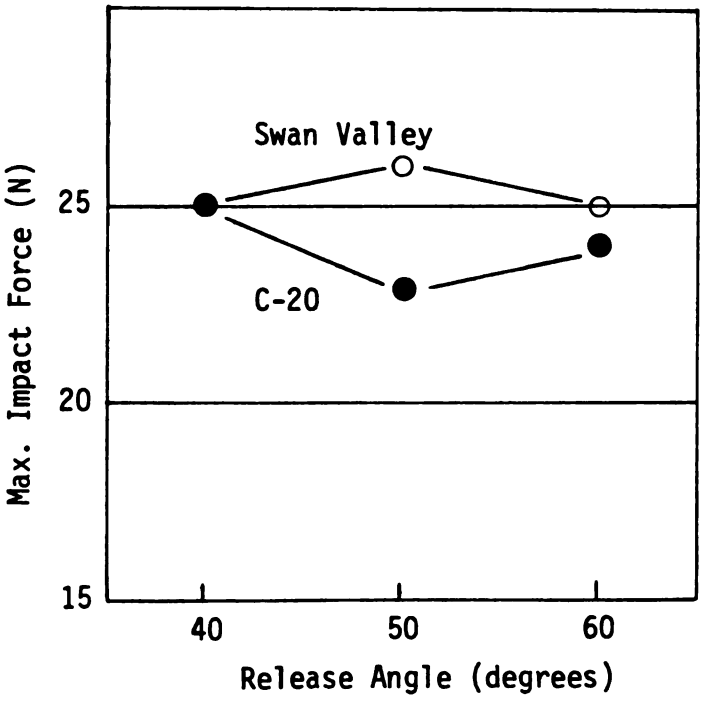

Figure 6.4 Interaction Between Variety and Release Angle For Maximum Impact Force

Table 6.8 Mean Maximum Impact Force (N) For All Samples

	1983	1984
grand mean	25.64	24.00
C-20	24.91	23.33
Swan Valley	26.36	24.66

shatter. Generally a higher moisture content increases the toughness of a seed (Srivastava et al., 1976 and Mensah et al., 1981). This is true for the Swan Valley bean pods which have a slightly higher moisture content than C-20. If we refer to Table 5.3 we may observe that the 1983 bean pods and seeds have an average of 13.5 percent w.b. moisture content compared to 14.6 percent w.b. for the 1984 samples. The drier pods seem to be tougher than the wet ones. Perhaps the difference in storage period and elapsed time after maturity may have a greater influence in causing the 1983 pods to be tougher than the 1984 pods.

Compression tests on 1983 Swan Valley bean pods using the Instron machine at Positions 1 and 2 give an average breaking force of 0.53 kgf (5.2 N) at a loading speed of 13 cm/min (5 in/min). Figure 6.5 shows the Instron output where the horizontal axis is load (kgf) and the vertical axis is the extension. The horizontal scale is 1 kgf per 5 cm (2 inches). These graphs suggest that the bean pod is weaker when hit on the side than on the pod suture (top). The compression tests gave an estimate of the force required to break the bean pods under slow loading but the maximum impact force to break bean pods was expected to be larger under fast loading than under slow loading (Mohsenin, 1978). The average impact force was found to be much greater than the breaking force under slow loading, as expected.

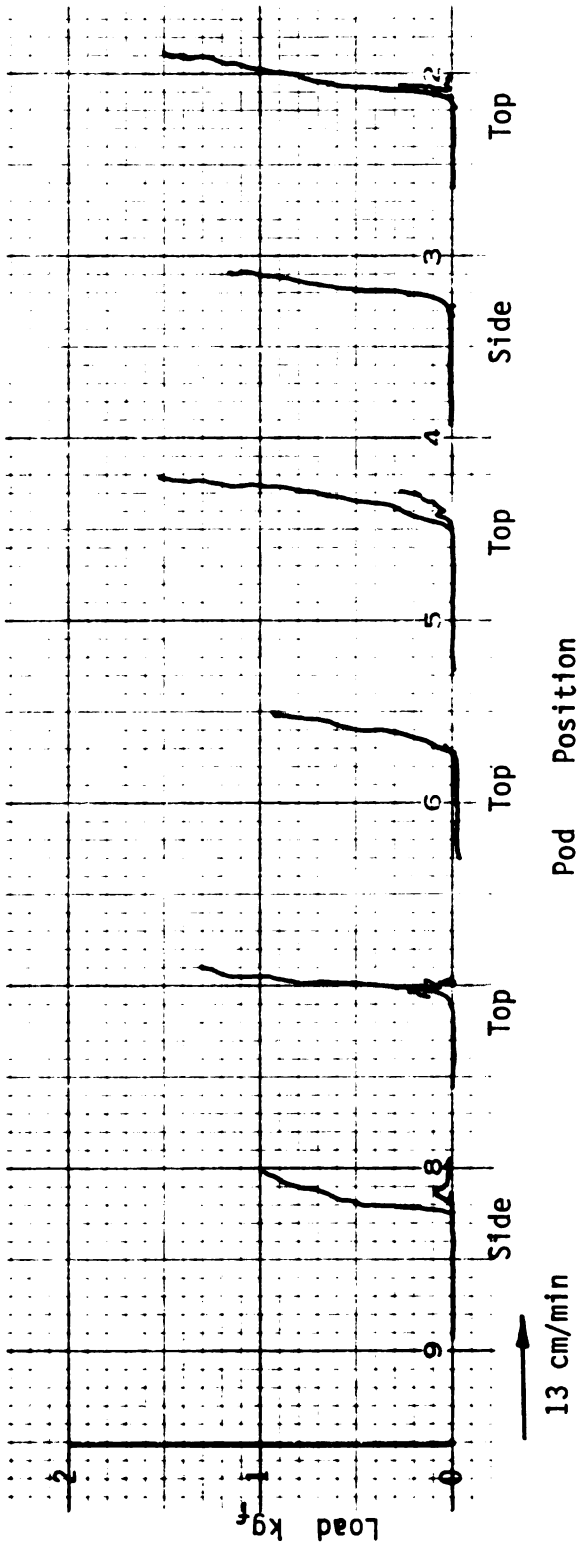

Figure 6.5 Output of Breaking Tests on the Instron Machine at 13 cm/minute (5 ipm) For Different Pod Positions

6.4 Absorbed Energy

The analysis of variance table for energy absorbed to shatter pods is given in Table 6.9. From Table 6.9, the statistical analysis suggests that the significant factors are release angle and pod position and the only significant interaction is the year-variety interaction. The plot of mean absorbed energy with release angle and pod position are shown in Figures 6.6 and 6.7 respectively. The mean absorbed energy values for different release angles are given in Table 6.10.

From Table 6.9 $s^2 = 48.7268$

$$s_d^2 = 2(s^2)/240$$

$$LSD = t_{\alpha/2} s_d$$

$$= 1.29$$

The results show that the mean absorbed energy at release angles of 50 and 60 are not significantly different at an α value of 0.05 but the mean absorbed energy for 40 degrees release angle is significantly smaller than for the other two release angles. The results indicate that some where between 40 and 50 degrees release angle a threshold input energy value is reached. At a release angle equal or greater than the threshold release angle, the energy absorbed by the bean pod remains the same.

The mean absorbed energy values for pod position are given in Table 6.11. Using the same LSD value as before

Table 6.9 Analysis of Variance for Absorbed Energy

Source	df	SS	MS	F
Rep(year)	2	143.705	71.853	1.4746 ns
Year	1	150.108	150.108	3.0806 ns
Variety	1	178.314	178.314	3.6590 ns
Angle	2	845.978	422.989	8.6808 **
Position	2	646.623	323.312	6.6352 **
Year-variety	1	243.420	243.420	4.9956 *
Year-angle	2	128.000	64.000	1.3134 ns
Year-position	2	236.594	118.297	2.4278 ns
Variety-angle	2	140.917	70.459	1.4460 ns
Variety-position	2	91.595	45.798	0.9399 ns
Angle-position	4	271.990	67.997	1.3955 ns
Year-variety -angle	2	155.342	77.671	1.5940 ns
Year-variety -position	2	55.927	27.964	0.5739 ns
Year-angle -position	4	170.439	42.610	0.8745 ns
Variety-angle -position	4	24.984	6.246	0.1282 ns
Year-variety -angle-position	4	126.530	31.633	0.6492 ns
Expt. error	34	1656.712	48.7268	
Sampling error	648	7212.160	11.1299	
Total	719	12479.353		

Note: 1. Rep(year) - replication within year
SS - Sum of Squares for deviations about a mean
df - Degree of freedom
MS - Mean Square i.e. Sum of Square divided by degrees of freedom
expt. - experimental

2. $F_{0.5}(1,30) = 4.17$
$F_{0.5}(2,30) = 3.32$
$F_{0.5}(4,30) = 2.69$

Table 6.10 Table of Means for Release Angle for Absorbed Energy

	Release Angle (degrees)		
	50	60	40
	11.24	10.56	8.68
40 deg	* 2.56	* 1.88	-
60 deg	0.68	-	
50 deg	-		

* significant at $\alpha = 0.05$

LSD = 1.29

Mean 50 deg	Mean 60 deg	Mean 40 deg
a	a	
		b

Underlined with same line do not have significant differences.

Mean 40 degrees = b

Mean 50 degrees = a

Mean 60 degrees = a

Table 6.11 Table of Means for Absorbed Energy for Pod Position

		Pod Position		
		Pos 1	Pos 2	Pos 3
		10.96	10.69	8.83
Pos 3	8.83	* 2.13	* 1.86	-
Pos 2	10.69	0.27	-	
Pos 3	10.96	-		

* significant at $\alpha = 0.05$

LSD = 1.29

Pos 1	Pos 2	Pos 3
a	a	
		b

Underlined with the same line are not significantly different.

Mean position 1 = a

Mean position 2 = a

Mean position 3 = b

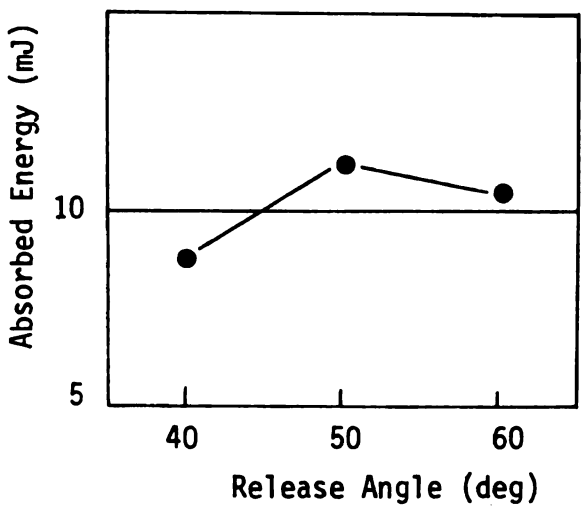

Figure 6.6 Plot of Mean Absorbed Energy With Release Angle

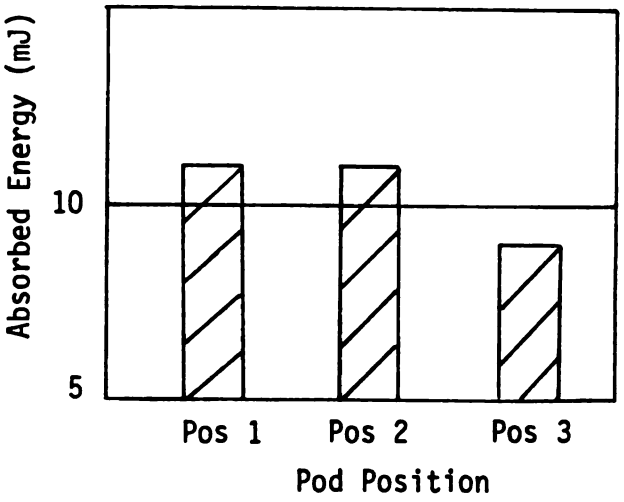

Figure 6.7 Plot of Mean Absorbed Energy With Pod Position

suggests that there is no significant difference between the mean absorbed energy for position 1 (side) and position 2 (top). The mean absorbed energy value for position 3 (bottom) is significantly smaller than for the other two pod positions. This result suggests that the bean pod is weakest along the base, and this is consistent with the results for impulse in Section 6.2. Table 6.12 shows the two-way table of means for year-variety interaction. The interaction is significant because the interaction value is greater than the LSD value. The performance for Swan Valley is about the same for the two years but the performance for the C-20 variety decreased for 1984. The plot of means for the year-variety interaction is given in Figure 6.8. The graphs support the statistical finding that the two varieties have different magnitudes of response for variety-year interactions.

From observation and literature (Hoag, 1972), the kinetic energy for the bean seeds are derived from two possible sources:

1. directly from the pendulum where energy is transferred to the seeds

2. energy stored in the bean pod, which is transferred from the pendulum when the pendulum deflects the bean pod, as strain energy. When the pod shatters, this strain energy is transferred to kinetic energy for the bean seeds.

Table 6.12 Table of Means for Year-Variety Interaction for Absorbed Energy

	Variety	
	C-20	Swan Valley
1983	11.70	9.54
1983	9.62	9.79

Main effect of variety = -.995

Main effect for year = -.915

Interaction between variety and year = 1.17

LSD = 1.05

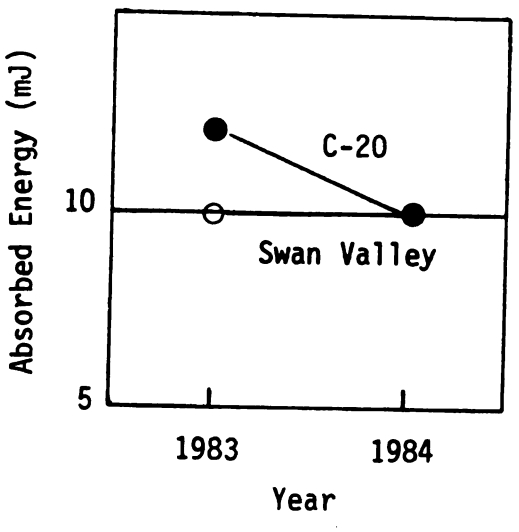

Figure 6.8 Interaction Between Year and Variety For Absorbed Energy

In this study the effects of storage time, elapsed time from maturity and moisture content are all confounded with year. The 1983 samples were taken from adjacent plots on the same afternoon. Given the same planting and harvesting time, the C-20 variety matures 4 days earlier than the Swan Valley variety. This characteristic is unique to C-20. The 1984 samples were taken not only 6 days apart, they were also taken from different locations. It is not clear whether both varieties have the same planting time or whether which variety has a longer elapsed time after maturity.

The 1983 samples were kept in storage for 16 months and the 1984 samples were kept for 4 months. The longer storage time may cause the 1983 sample to be drier and tougher. This is evident from the higher maximum impact force values for the 1983 bean pods which had the lower moisture level. In reality moisture content also depends on upon the past weather conditions and upon the transfer characteristics of the plant (Hoag, 1975). Together with the effects of storage time, elapsed time after maturity and varietal differences, the effect of moisture content on the performance of the bean pods is not clear. Within variety the effects of moisture content and maturity effects are also confounded. To conserve the moisture content of the bean pods, the samples were stored in two layers of plastic bags in the refrigerator as soon as they

were taken to the laboratory, and one bean pod at a time was taken out of the sealed bag with reseal for impaction.

The experimental error for all measurements of impulse, maximum impact force and energy absorbed to shatter were larger than the residual error obtained from the SPSS program. The large experimental error may be due to different sample locations. As mentioned above there are many confounding effects within year as well as variety and these may also contribute to the experimental error.

The results suggest that impulse is the most suitable parameter to characterize impact resistance for navy bean pods because it is independent of variety, harvest time and impact velocity. Although absorbed energy depends on release angle and pod position as main effects, it is not the most suitable parameter because of the significant year-variety interaction. Hoag (1975) worked on impact testing of soybean pods, he also found impulse, compared with maximum impact force and energy absorbed, to be the most suitable parameter to characterize impact resistance.

6.5 Summary

Absorbed energy, maximum impact force and impulse values were computed for C-20 and Swan Valley varieties. The grand mean values are as follows: mean energy is 10.16 mJ, range 1.40 - 31.50 mJ; mean maximum impact force is

24.82 N, range 11.32 - 36.97 N; and mean impulse is 24.32 N-ms, range 6.04 - 71.67 N-ms. The threshold release angle for absorbed energy lies between 40 and 50 degrees. Impulse is the most suitable parameter to characterize impact resistance because it is independent of variety, harvest time and release angle. Impulse is only dependent on the orientation of the bean pod. The LSD procedure shows that the bean pod is strongest when hit on the side and weakest when hit at the base. Varietal and age of bean pod differences are significant in the calculation of maximum impact force.

CHAPTER VII

CONCLUSIONS AND SUGGESTIONS

7.1 Conclusions

The following conclusions were reached in this study.

1. The mean absorbed energy is 10.16 mJ with a range of 1.40 - 31.50 mJ. The mean maximum impact force is 24.82 N with a range of 11.32 -36.97 N. The mean impulse is 24.32 N-ms with a range of 6.04 - 71.67 N-ms.

2. Both impulse and absorbed energy to shatter depend on pod position. Both results show that the bean pod is weakest when hit along the base. For impulse all three pod positions have significantly different when using the LSD procedure with the pod strongest when hit on the side. The absorbed energy is not significantly different when the pod is hit on the side and at the pod suture (top).

3. Impulse is the most suitable parameter to characterize impact resistance because it is independent of variety, age of bean pods in storage and pendulum

release angles.

4. Varietal and age differences are significant for maximum impact force. Both C-20 and Swan Valley perform differently under the same conditions, Swan Valley has a mean maximum impact force of 25.51 N and C-20 has a mean value of 24.12 N.

5. The threshold pendulum release angle for absorbed energy lies between 40 and 50 degrees.

7.2 Suggestions

The following suggestions were made for further study.

1. Further investigations on the effect of moisture content on impulse, maximum impact force and absorbed energy and their interactions with storage time, and elapsed time after maturity of the bean pods.

2. Further investigations on the cyclic effect of moisture content. We may start with wet bean pods, perform impact tests as the moisture content reduces, then apply moisture to the bean pods to come back to the initial moisture levels.

3. Further investigations on the effect of bean pod length. Preliminary tests have indicated variable

performance when the bean pod is hit on different positions along the bean pod.

4. Investigate properties of the bean pod as a storage for strain energy, and the twisting effect of the bean pod valves, the direction and the magnitude of the forces which cause the twisting effect.

5. Determine the threshold release angle for absorbed energy.

6. When conducting experimental work on biological products, the harvest time, and maturity time must be noted. Knowledge of the product moisture content at harvest should be helpful to the experimental work.

BIBLIOGRAPHY

BIBLIOGRAPHY

Adams, A.W., 1981 Update: New Bean Architype. Michigan Dry Bean Digest 5(2):12-13, 20.

Affeldt, Henry A., Jr., 1984 Digital Analysis of the Dynamic Response Within Trunk Shaker Harvester Systems. Michigan State University. M.S. Thesis.

Bilanski, W.K., 1966 Damage Resistance of Seed Grains. Transactions of the ASAE 9(3): 360-363.

Bledsoe, B.L. and Homer D. Swingle, 1972 Detachment Properties of Snap Beans. Transactions of the ASAE 15(6): 1174-1178.

Bracegirdle, B. and P.H. Miles, 1973 An Atlas of Plant Structure Volume 2. Heinemenn Educational Books Ltd. London.

Burkhardt, T.H. and B.A. Stout, 1971 A High-Velocity, High-Momentum Impact Testing Device for Agricultural Materials. Transactions of the ASAE 14(3): 455-457.

Burkhardt, T.H. and B.A. Stout, 1974 Laboratory Investigations of Corn Shelling Utilizing High-Velocity Impact Loading. Transactions of the ASAE 17(1): 11-14.

Cooke, J.R. and James Dickens, 1971 Centrifugal Gun for Impaction Testing of Seeds. Transactions of the ASAE 14(1): 147-155.

Dally, J.W. and W.F. Riley, 1978 Experimental Stress Analysis. Mc Graw Hill Book Company, New York.

Doebelin, Ernest O., 1975 Measurement Systems Application and Design. Mc Graw Hill Book Company, New York.

Esau, Katherine, 1953 Plant Anatomy. John Wiley and Sons Inc, New York.

Esau, Katherine, 1960 Anatomy of Seed Plants. John Wiley and Sons Inc, New York.

Finney, Essex E., Jr. and David R. Massie, 1975 Instrumentation for Testing the Response of Fruits to Mechanical Impact. Transactions of the ASAE 18(6):

1184-1187, 1192.

Fluck, Richard, C. and Esam Ahmed, 1973 Impact Testing of Fruits and Vegetables. Transactions of the ASAE 16(4): 660-666.

Ghate, Suhas R. and R.P. Rohrbach, 1975 Mechanical Properties Influencing Vibrations in Blueberry Canes. Transactions of the ASAE 18(5): 921-925, 931.

Goldsmith, W., 1960 Impact- The Theory and Physical Behavior of Colliding Solids. Edward Arnolds (Publishers) Ltd., London.

Goyal, Megh R., L.O. Drew, G.L. Nelson, T.J. Logan, 1980 Critical Time for Soybean Seedling Emergence Force. Transactions of the ASAE 23(4): 831-839.

Gunkel, W.W. and L.L. Anstee, 1962 Direct Harvesting of Dry Beans. Agricultural Engineering 43(12): 694-716.

Hammerle, J.R. and N.N. Mohsenin, 1966 Some Dynamic Aspects of Fruit Impacting Hard and Soft Materials. Transactions of the ASAE 9(4): 484-488.

Hoag, Dean L., 1972 Properties Related to Soybean Shatter. Transactions of the ASAE 15(3): 494-497.

Hoag, Dean L., 1975 Determination of the Susceptibility of Soybeans to Shatter. Transactions of the ASAE 18(6): 1174-1179.

Hoki, Makoto O., 1973 Mechanical Strength and Damage Analysis of Navy Beans. Ph.D. Dissertation. Michigan State University.

Hoki, M. and L.K. Pickett, 1973 Factors Affecting Mechanical Damage of Navy Beans. Transactions of the ASAE 16(6): 1154-1157.

Hummel, J.W. and W.R. Nave, 1976 Cutting of Soybean Plants. Transactions of the ASAE 19(1): 35-39.

Idell, J.H., R.G. Holmes and E.G. Humphries, 1975 Strawberry Resonance Frequencies and Drag Coefficients in Relation to an Air Suspension-Stem Vibration Harvesting System. Transactions of the ASAE 18(3): 427-430.

Keller, Duane L., H.H. Converse, T.O. Hodges and Do Sup Chung, 1972 Corn Kernel Damage Due to High Velocity Impact. Transactions of the ASAE 15(2): 330-332.

Kelly, J., T. Burkhardt, G. Varner, W. Adams and A. Srivastava, 1981 Comparison of Dry Bean Harvesting Methods. Report to Michigan Dry Bean Production Research Advisory Board. Michigan State University. Unpublished.

Kelly, J.D. and A.W. Adams, 1981 Bean Comparisons - Newly Developed and Traditional Bean Plant Types for Michigan. Michigan Dry Bean Digest 6(1): 14, 24.

Kelly, J.D., 1984 Personal Communication.

Khan, Amir U., 1952 Efficiency of Harvesting Navy Beans With a Combine. M.S. Thesis. Michigan State University. Unpublished.

Lyon, R.L. and J.L. Zable, 1973 Impact-Force Source and Impact-Force Calibrator. Experimental Mechanics 6(13): 257-264.

Mc Colly, H.F., 1958 Harvesting Edible Beans in Michigan. Transactions of the ASAE 1(1): 68-75.

Measurements Group Tech Note TN-502, 1979 Raleigh, North Carolina.

Measurements Group Tech Note TN 128-3, 1976 Rayleigh, North Carolina.

Mensah, J.K., F.L. Herum, J.L. Blaisdell and K.K. Stevens, 1981 Effect of Drying Conditions on Impact Shear Resistance of Selected Corn Varieties. Transactions of the ASAE 24(6): 1568-1572.

Michigan Agricultural Statistics, 1984 Michigan Department of Agriculture, page 5, 14.

Mohsenin, N,N., 1978 Physical Properties of Plant and Animal Materials. Gordon and Breach Science Publishers Inc., New York.

Narayan, C.V., 1969 Mechanical Checking of Navy Beans. Ph.D. Dissertation. Michigan State University.

Paulsen, M.R., W.R. Nave and L.E. Gray, 1981 Soybean Seed Quality as Affected by Impact Damage. Transactions of the ASAE 24(6): 1577-1582, 1589.

Perry, J.S. and C.W. Hall, 1965 Mechanical Properties of Pea Beans Under Impact Loading. Transactions of the ASAE 8(2): 191-193.

Perry, J.S. and C.W. Hall, 1966 Evaluating and Reducing Mechanical Handling Damage to Pea Beans. Transactions of the ASAE 9(5): 696-701.

Pickett, Leroy K., 1973 Mechanical Damage and Processing Loss During Navy Bean Harvesting. Transactions of the ASAE 16(6): 1047-1050.

Pickett, Leroy K., 1982 Harvesting Dry Beans. Dry Bean Production - Principles and Practices, edited by L.S. Robertson and R.D. Frazier. Cooperative Extension Service, Agricultural Experimental Station. Michigan State University.

Rohrbach, R.P. and S.W. Glass, 1980 Driving Point Mechanical Impedance of Blueberries. Transactions of the ASAE 23(2): 298-302.

Sharma,R. and W. Bilanski, 1971 Coefficient of Restitution of Grains. Transactions of the ASAE 14(2): 216-218.

Singh, Bachchan, 1975 Environmental Effects on Navy Bean Field Drying and Harvesting. Ph.D. Dissertation. Michigan State University.

Singh, S.S. and M.F. Finner, 1983 A Centrifugal Impactor for Damage Susceptibility Evaluation of Shelled Corn. Transactions of the ASAE 26(6): 1858-1863.

Srivastava, A.K., F.L. Herum and K.K. Stevens, 1976 Impact Parameters Related to Physical Damage to Corn Kernel. Transactions of the ASAE 19(6): 1147-1151.

Turner, W.K., C.W. Suggs and J.W. Dickens, 1967 Impact Damage to Peanuts and Its Effects on Germination, Seed Development, and Milling Quality. Transactions of the ASAE 10(2): 248-251.

Weeks, S.A., J.C. Wolford and R.W. Kleis, 1975 A Tensile Method for Determining the Tendency of Soybean Pods to Dehisce. Transactions of the ASAE 18(3): 471-481.